BEILSTEIN JOURNAL OF ORGANIC CHEMISTRY

Young investigators in earth-abundant metal catalysis

Edited by Guillaume Lefèvre and L. Reginald Mills

Generated on 23 November 2026, 03:36

Imprint

Beilstein Journal of Organic Chemistry
www.bjoc.org
ISSN 1860-5397
Email: journals-support@beilstein-institut.de

The *Beilstein Journal of Organic Chemistry* is published by the Beilstein-Institut zur Förderung der Chemischen Wissenschaften.

Beilstein-Institut zur Förderung der Chemischen Wissenschaften
Trakehner Straße 7–9
60487 Frankfurt am Main
Germany
www.beilstein-institut.de

The copyright to this document as a whole, which is published in the *Beilstein Journal of Organic Chemistry*, is held by the Beilstein-Institut zur Förderung der Chemischen Wissenschaften. The copyright to the individual articles in this document is held by the respective authors, subject to a Creative Commons Attribution license.

BEILSTEIN JOURNAL OF ORGANIC CHEMISTRY

CO_2 silylation at a tucked-in iron(II) complex

Logan J. Taylor and Marcus W. Drover*

Full Research Paper

Open Access

Address:
Department of Chemistry, Western University, 1151 Richmond Street, London, ON, N8K 3G6, Canada

Email:
Marcus W. Drover* - marcus.drover@uwo.ca

* Corresponding author

Keywords:
carbon dioxide; iron; organometallics; silylation; tucked-in complex

Beilstein J. Org. Chem. **2026,** *22,* 1295–1302.
https://doi.org/10.3762/bjoc.22.104

Received: 24 July 2026
Accepted: 11 September 2026
Published: 23 September 2026

This article is part of the thematic issue "Young investigators in earth-abundant metal catalysis".

Guest Editor: G. Lefevre

© 2026 Taylor and Drover; licensee Beilstein-Institut.
License and terms: see end of document.

Abstract

Carbon dioxide (CO_2) capture and valorization remain central challenges in sustainable chemistry due to the persistence of CO_2 as a major greenhouse gas. Herein, we describe the functionalization of a CO_2-activated organometallic complex, [(Cp*–CO_2)Fe(diphosphine)] (**1**; Cp* = C_5Me_5) in which CO_2 is selectively incorporated into the Cp* ligand framework. Treatment of **1** with trimethylsilyl chloride (TMSCl) affords [{Cp*–C(O)–O–TMS}Fe(diphosphine)Cl] (**2**) via silylation of the Fe–O(CO_2) linkage. Chloride abstraction using $NaBPh_4$ generates the putative complex [{Cp*–C(O)–O–TMS}Fe(diphosphine)]$^+$ (**3**), featuring a labile dative $R_2C{=}O{\rightarrow}Fe$ interaction that is readily displaced by acetonitrile to give [{Cp*–C(O)–O–TMS}Fe(diphosphine)($NCCH_3$)]$^+$ (**4**). Reduction of the ester functionality in **2** using $HBCy_2$ (Cy = cyclohexyl) provides access to new borylated complexes. Collectively, these results demonstrate the cooperative capture and stepwise CO_2 functionalization at a common Cp* ligand framework.

Introduction

Carbon dioxide (CO_2) is a prominent greenhouse gas generated by many natural pathways, including animal respiration and plant death [1], but also increasingly through industrial processes such as the burning of fossil fuels [2]. Greenhouse gases are characterized by their inability to escape Earth's atmosphere, which in turn prevents the escape of heat – a key contributor to climate change [3]. Fossil fuel-derived CO_2 emissions continue to increase, with approximately 43% of annual CO_2 emissions remaining in the atmosphere; this has led to a growing interest in CO_2 remediation strategies [2]. Organometallic compounds are well-known for their use in CO_2 activation, with examples spanning the s- [4,5], p- [6], d- [7,8], and f-blocks [9]. For d-block elements, examples include early [9] to late transition metals [10], with ongoing efforts focused on optimizing CO_2 conversion catalysis [11,12] into useful products, such as CO, formaldehyde, methanol, and more [6,9,10].

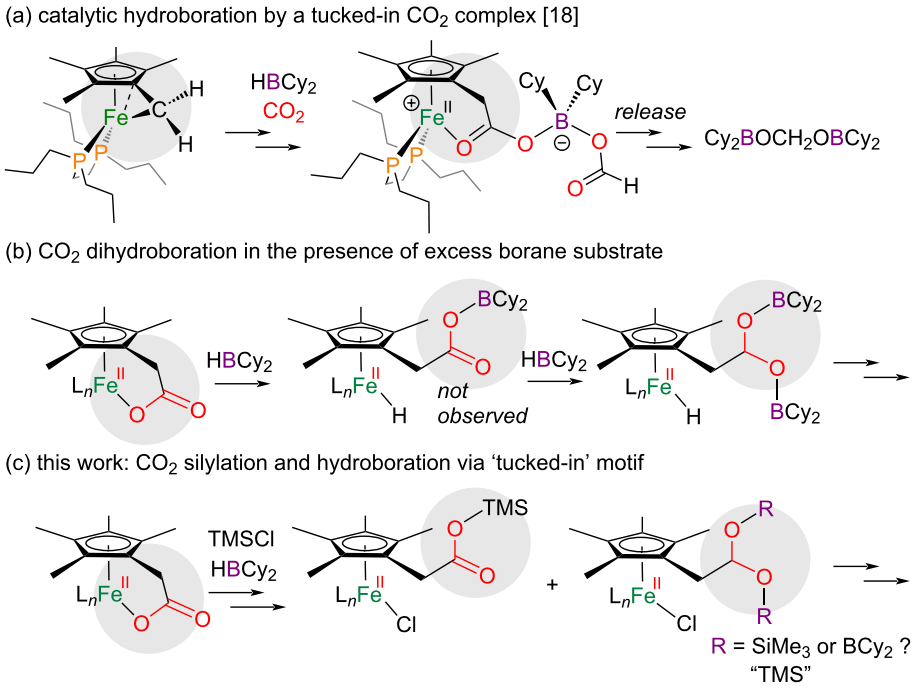
Of reduction strategies, examples of CO_2 hydroboration and hydrosilylation to give bisboryl or silyl ethers have been achieved, which once hydrolyzed provide access to C1-containing synthons. CO_2 hydroboration has been demonstrated using

a wide range of metals including manganese [13], nickel [14], and palladium [14] to generate borylated analogues of methanol, with various reagents such as pinacolborane (HBPin) [13] and 9-borabicyclo[3.3.1]nonane (9-BBN) [13,14]. Metal-free examples using p-block elements such as silicon [15] and nitrogen [16] have also been shown. Recently, our group contributed to this space, reporting a tucked-in iron complex that reacts with CO_2 to give a ferralactone (Scheme 1a and b) [17] which undergoes addition of dicyclohexylborane ($HBCy_2$) to give [(Cp*–BCy_2)Fe(diphosphine)H] – a competent catalyst for CO_2 dihydroboration using $HBCy_2$ [18]. We suggest this reaction occurs via a CO_2 B–O templating strategy using a pendent secondary coordination sphere (SCS) borane moiety [18].

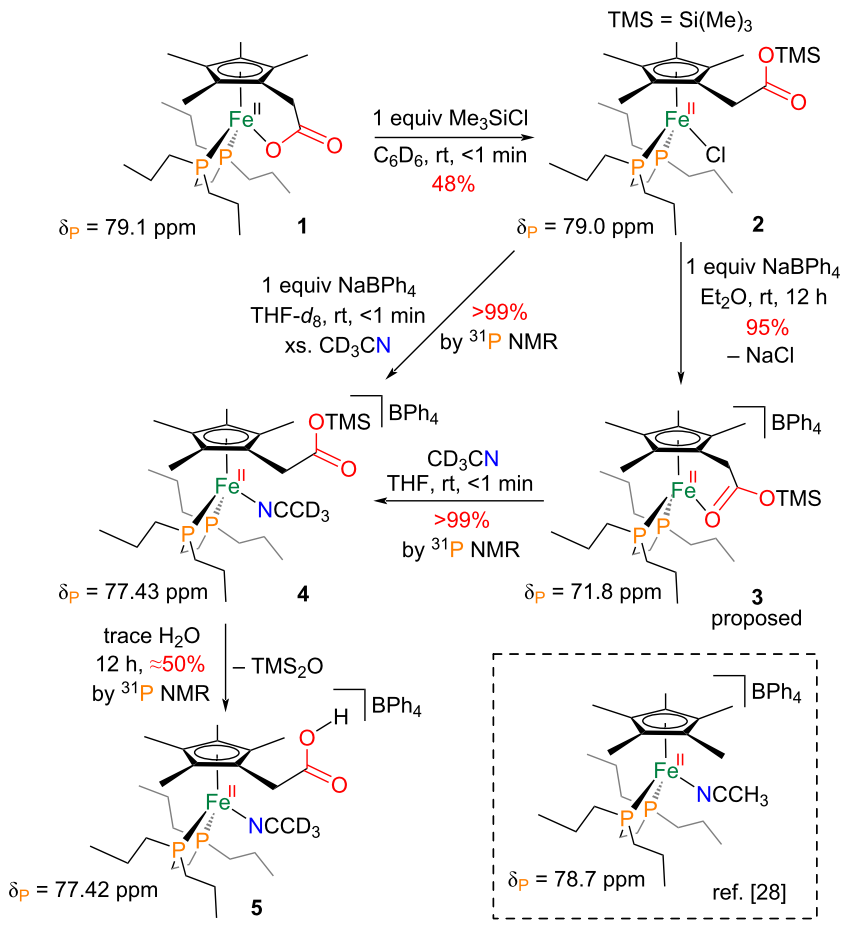
CO_2 (hydro)silylation is complementary to hydroboration, leading to the formation of robust Si–O bonds. Indeed, Leitner and co-workers demonstrated that a cobalt–triazine complex can catalytically produce silylated analogues of formate, methanol, and formaldehyde in the presence of silane, with product selectivity depending on the reaction temperature [19]. Iron has also been shown to hydrosilylate CO_2 by Cantat and co-workers, who used different iron(II) phosphine salts to generate formamides and methylamines in the presence of different amines [20]. Other contributions using cobalt pincer complexes [21], NHC-stabilized (NHC = N-heterocyclic carbene) stannyliumylidene complexes [22], and oxorhenium tridentate PNN catalysts [23] to reduce CO_2 have also been established. Relevant to this work, a 2022 report by Horáček demonstrated the silylation of CO_2 using a titanium 'tucked-in' compound in combination with trimethylsilyl chloride (TMSCl) [24]. Building on these precedents, we sought insight into the reactivity of [(Cp*–CO_2)Fe(diphosphine)] with a silyl electrophile. The unusual CO_2-functionalized Cp*Fe framework provides a rare platform for interrogating how tucked-in motifs participate in reductive transformations with silanes. These studies complement our prior work on hydroboration (Scheme 1b and c) and aim to elucidate broader patterns in base-metal-mediated CO_2 reduction chemistry.

Results and Discussion

To begin, [(Cp*–CO_2)Fe(d*n*ppe)] (**1**) [17] was prepared by reaction of the tucked-in complex, [(η^6–C_5Me_4–CH_2)Fe^{II}(d*n*ppe)] with 1 atm of CO_2 at room temperature. Complex **1** has a characteristic ^{31}P NMR spectroscopic signature at δ_P = 79.1 ppm and a distinct ν(CO) stretch at 1622 cm^{-1}. Treatment of **1** with 1 equiv of trimethylsilyl chloride (TMSCl) yielded a slightly darker purple solution, with a very similar $^{31}P\{^1H\}$ NMR shift to **1** at δ_P = 79.0 ppm, which mirrors the value observed for the known complex [Cp*Fe(d*n*ppe)Cl] (δ_P = 79.4 ppm) (Scheme 2) [25]. Of note, both complex **1** and its tucked-in precursor show no productive reactivity with hydridosilanes such as Ph_3SiH. By ^1H,^{29}Si HMBC NMR spectroscopy, TMS incorporation was corroborated by the presence of a cross-signal at δ_H = 0.22 ppm



Scheme 1: (a) Catalytic hydroboration by a tucked-in CO_2 complex ([18]); (b) CO_2 dihydroboration in the presence of excess borane substrate; (c) this work: CO_2 silylation and hydroboration via 'tucked-in' motif.



Scheme 2: Synthesis of the silylated CO_2 adduct **2** and subsequent chloride abstraction.

(9H) and δ_{Si} = −24 ppm, indicating formation of [{Cp*–C(O)–O–TMS}Fe(d*n*ppe)Cl] (**2**), having a peripherally silylated CO_2 group. Further examination of the ^{1}H NMR spectra confirms C_s symmetry, rendering the functionalized CH_2 protons equivalent (δ_H = 3.49 ppm) (Figure 1a). By LIFDI–MS, **2** displays a molecular ion at *m/z* = 604.2474 (calcd. *m/z* = 604.2485 for $C_{28}H_{55}O_2ClFeP_2Si$). The structure of **2** was further confirmed by scXRD using purple crystals grown from a saturated pentane solution at −35 °C. The solid-state structure reveals an Fe–Cl bond length of 2.353(1) Å and a Si–O bond length of 1.699(2) Å (Figure 1a, inset). The silylated ester fragment exhibits bond metrics of r(C–C(O)) = 1.509(3) Å, r(C=O) = 1.207(2) Å, and r(C–O) = 1.346(3) Å. The lengths of the C–O and C=O bonds fall within the expected literature range for ester functional groups of 1.35–1.40 Å and 1.1–1.2 Å, respectively [26].

Motivated by the clean silylation reactivity of **1**, we explored whether removal of the iron-bound Cl ligand in **2** could promote onwards reactivity, potentially enabling interaction between the Fe center and the C=O group. As such, **2** was reacted with sodium tetraphenylborate ($NaBPh_4$) in diethyl ether over 12 hours, affording a cloudy yellow solution. Subsequent analysis by $^{31}P\{^1H\}$ NMR spectroscopy revealed a broad peak at δ_P = 71.8 ppm ($\Delta_{1/2}$ = 60 Hz), suggestive of abstraction (Figure 1b). The width of this resonance suggested an equilibrium involving [{Cp*–C(O)–O–TMS}Fe(d*n*ppe)]$^+$, potentially between a carbonyl oxygen-bound and unbound form, or between the bound species and its dinitrogen adduct [{Cp*–C(O)–O–TMS}Fe(d*n*ppe)(N_2)]$^+$ (δ_P = 71.2 ppm for [Cp*Fe(d*n*ppe)(N_2)]$^+$, for example). The unbound (N_2-free) species adopts a triplet electronic configuration (*S* = 1) and is higher in energy than its corresponding N_2 adduct (*S* = 0) [27]. These possibilities prompted further investigation by variable-temperature NMR spectroscopy (Figure 1b). Upon cooling to −75 °C, this ^{31}P NMR peak significantly sharpens and moves to δ_P = 73.5 ppm, which is attributed to the coordination equilibrium, as described above. Further supporting an "on–off" equilibrium in **3**, introduction of the weak L–type donor, acetonitrile, provided a ^{31}P NMR resonance at

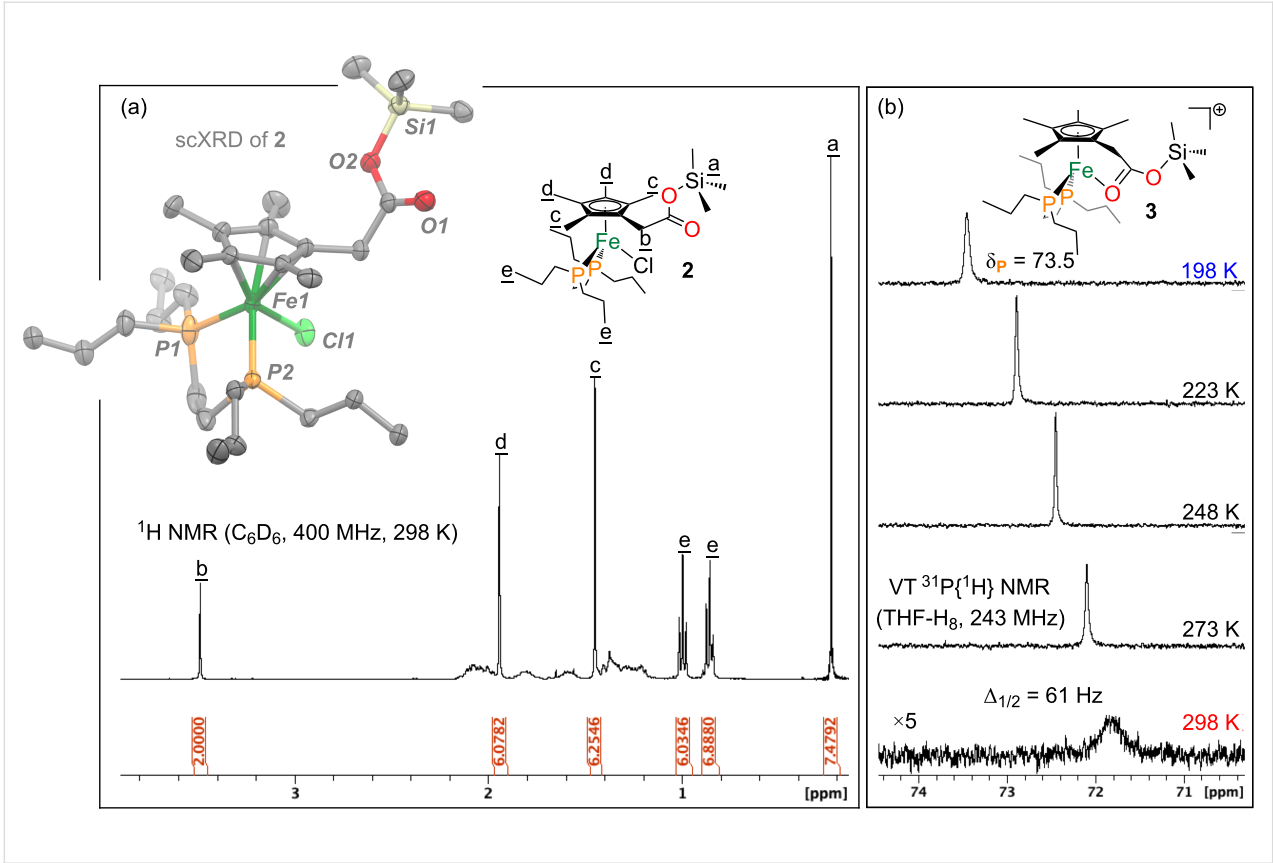
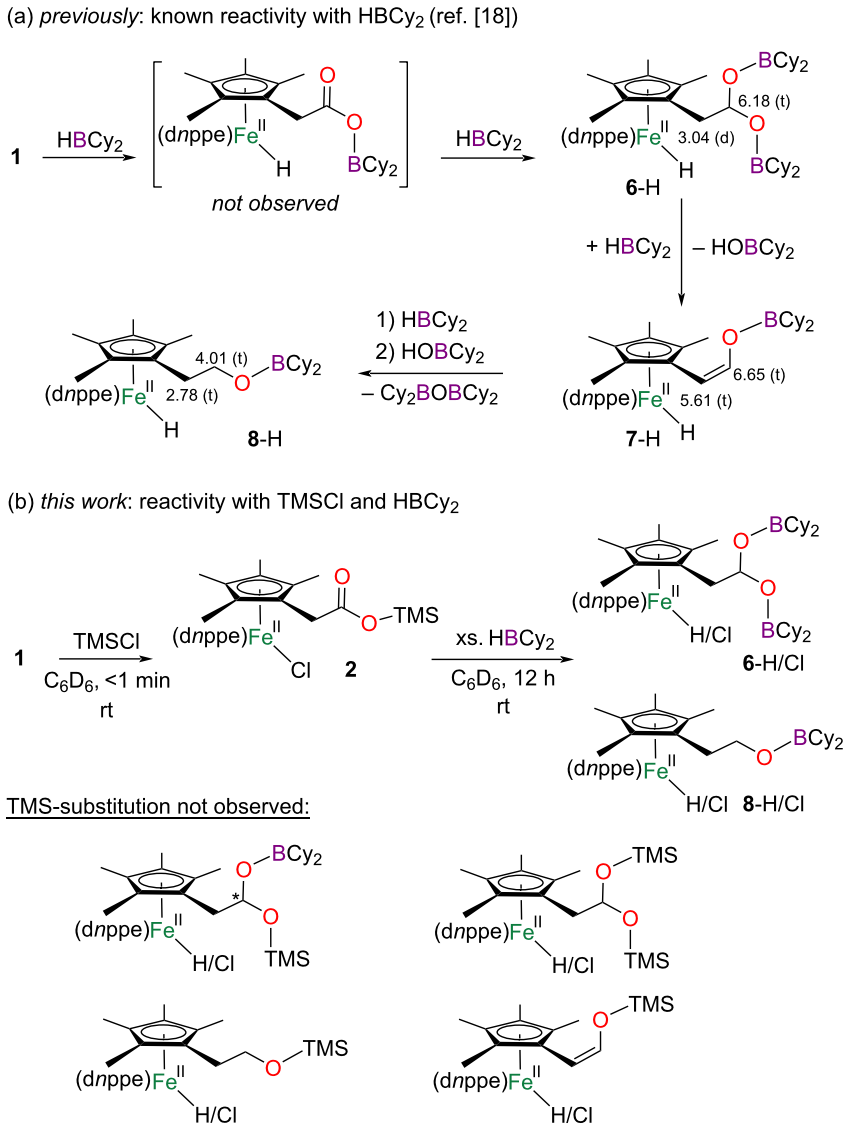


Figure 1: (a) **2**, ^{1}H NMR, C_6D_6, 400 MHz, 298 K. Inset shows the molecular structure of **2** with ellipsoids drawn at 50% probability. Hydrogen atoms are omitted for clarity; (b) variable-temperature (VT) ^{31}P{^{1}H} NMR for **3** from 298 to 198 K (THF-H_8, 243 MHz). Broad signals in ^{1}H NMR baseline of **2** attributed to d*n*ppe CH_2 signals.

δ_P = 77.4 ppm; this is similar to the model complex, $[Cp^*Fe(dnppe)NCCH_3]^+$ (δ_P = 78.7 ppm) [28], suggesting formation of $[\{Cp^*–C(O)–O–TMS\}Fe(dnppe)NCCH_3]^+$ (**4**) and displacement of the weak $R_2C{=}O{\rightarrow}Fe$ interaction (Scheme 2). During efforts to characterize **4**, desilylation occurred, likely due to the presence of trace amounts of moisture in the THF or MeCN used, giving **5** (δ_H = 11.1 ppm) and 0.5 equiv TMS_2O (δ_H = 0.07 ppm) [29] (see Supporting Information File 1). By ESI–MS, **5** displays an $[M - H]^+$ signal at *m*/*z* = 496.2309 (calcd. *m*/*z* = 496.2322 for $C_{25}H_{46}FeO_2P_2$); a signal for **4** was not observed, again highlighting the ease by which the –OTMS group is cleaved.

Like **1**, complex **2** also undergoes reduction upon treatment with excess $HBCy_2$. Multinuclear NMR spectroscopic analysis supports the formation of several C_2-functionalized Cp* compounds, including the bisborylacetal (**6**–H), vinyloxyborane (**7**–H), and ethoxyborane (**8**–H) complexes where X–H refers to an {Fe–H} species; these were identified in the crude reaction mixture based on characteristic NMR signatures (Scheme 3) and from our previous work independently reacting **1** with $HBCy_2$ [18]. These products arise from successive borane additions to the CO_2-derived C_2 unit, ultimately leading to the formation of ethoxyborane complex **8**–H. Unlike **1**, the use of the {Fe–Cl} precursor **2** further complicates analysis of the product mixture, possessing several {Fe–Cl}-containing species (X–Cl) in addition to {Fe–H}-containing complexes **6**–H and **8**–H. By LIFDI–MS of the product mixture, two predominant signals are seen at *m*/*z* = 660.4416 (calcd. 660.4423 for $C_{37}H_{71}OBFeP_2$ for **8**–H) and *m*/*z* = 694.4025 (calcd. 694.4033 for $C_{37}H_{70}OBClFeP_2$ for **8**–Cl). Consistent with the strong leaving ability of –OTMS, silylated Cp* complexes were not observed by crude ^{1}H NMR spectroscopy nor LIFDI–MS. The fate of $–SiMe_3$ was not determined, however, TMS signals could be observed between 0.1–0.3 ppm via ^{1}H NMR spectroscopy. Formation of Me_3SiH during the synthesis of **6**–H/Cl is possible, however, it is highly volatile (bp 6.7 °C) [30], and a characteristic multiplet ($\delta_{Si–H} \approx 4.0$ ppm) [31] was not observed by ^{1}H NMR spectroscopy.

Overall, this reductive chemistry provides a route to Cp* products in which CO_2 serves as a C1 synthon at a silylated iron complex, enabling access to reduced ethyl-functionalized derivatives, albeit with lower selectivity for iron hydride products



Scheme 3: Observed reactivity between **1**, TMSCl, and $HBCy_2$. Numbers refer to ^1H NMR shifts (multiplicity).

when compared to previous results using hydroboration of **1** [18].

Conclusion

In summary, we have demonstrated that a CO_2-functionalized tucked-in iron complex can be stepwise derivatized. Electrophilic silylation with TMSCl functionalizes the Fe–CO_2 linkage to afford a silyl ester. Subsequent chloride abstraction suggests generation of a cationic complex featuring a weak, fluxional intramolecular carbonyl O→Fe interaction that is readily displaced by the neutral donor ligand, acetonitrile, highlighting the hemilabile nature of the tethered ester functionality. Preliminary hydroboration studies further demonstrate that the silylated CO_2 fragment remains susceptible to downstream desilylation and reduction. Collectively, these results provide new opportunities for the development of organometallic strategies that combine CO_2 activation with selective C_1–derivatization.

Experimental

General considerations

All experiments were carried out employing standard Schlenk techniques under an atmosphere of dry nitrogen employing degassed, dried solvents. Benzene and THF were tested with a standard purple solution of sodium benzophenone ketyl in tetrahydrofuran to confirm effective moisture removal. Acetonitrile was dried over molecular sieves and degassed by three freeze–pump–thaw cycles [32]. All other reagents were pur-

chased from commercial vendors and used without further purification unless otherwise stated. [(Cp*–CO_2)Fe(d*n*ppe)] (**1**) was prepared according to literature procedures [17].

Physical methods

All NMR data were recorded with a Bruker AVIII HD 400 MHz, a Bruker Neo 600 MHz, or a Varian INOVA 600 instrument. ^{1}H NMR spectra are reported in parts per million (ppm) and are referenced to residual solvent, e.g., ^{1}H (C_6D_6): δ = 7.16; ^{13}C (C_6D_6): δ = 128.06; coupling constants are reported in Hz. ^{11}B, ^{13}C, ^{29}Si, and ^{31}P NMR spectra were performed as proton-decoupled experiments (unless explicitly stated otherwise) and are reported in ppm. Selective irradiation experiments (^{1}H 1D TOCSY) were performed by selective irradiating signal of interest using a Bruker Neo 600 MHz instrument. 2D NMR experiments (^{1}H,^{1}H COSY, ^{1}H,^{13}C HSQC) were run using standard acquisition parameters on a Bruker Neo 600 MHz instrument. ^{1}H,^{29}Si HSQC was performed with a Bruker AVIII HD 400 MHz instrument. VT ^{31}P{^{1}H} NMR was performed with a Varian INOVA 600 instrument. Mass spectrometry was carried out with a Thermo Scientific Orbitrap Exploris 120 Instrument.

Preparation of compounds

[(η^5–C_5Me_4–CH_2–$CO_2Si(CH_3)_3$)Fe(d*n*ppe)Cl] (**2**; $C_{28}H_{55}FeO_2P_2ClSi$, MW = 604.6 g/mol): In a glovebox, **1** (23 mg, 0.046 mmol) was dissolved in benzene (2 mL) in a 20 mL scintillation vial. Trimethylsilyl chloride (5.89 µL, 0.046 mmol) was added and the reaction occurred immediately. The mixture was then washed three times with pentane (3 × 2 mL) and filtered through Celite® 545. Removal of volatiles in vacuo gave **2** as a purple solid (11.4 mg, 48%).^{1}H NMR (400 MHz, C_6D_6, 298 K) δ_H 3.49 (s, 2H, η^5-C_5Me_4-(CH_2)), 2.09 (m, 6H, overlapping CH_2 signals), 1.94 (s, 6H, η^5-C_5Me_4-(µ-CH_2)), 1.83 (m, 2H, CH_2), 1.59 (m, 2H, CH_2), 1.45 (s, 6H, η^5-C_5Me_4-(µ-CH_2)), 1.30 (m, 10H, CH_2 signals), 0.99 (t, $J_{H,H}$ = 7.2 Hz, 6H, P-CH_2-CH_2-CH_3) 0.85 (t, $J_{H,H}$ = 7.2 Hz, 6H, P-CH_2-CH_2-CH_3), 0.22 (s, 9H, Si-(CH_3)$_3$); ^{31}P{^{1}H} NMR (162 MHz, C_6D_6, 298 K) δ_P 79.0 ppm; ^{1}H,^{29}Si NMR HMBC (400 MHz, C_6D_6, 298 K) δ_{Si} −24 ppm; ^{13}C{^{1}H} NMR (101.5 MHz, C_6D_6, 298 K) δ_C 171.7 (s, C_5Me_4-CH_2-*C*O_2), 86.1 (s, *C*$_5$Me$_4$-CH_2-CO_2), 79.9 (s, *C*$_5$Me$_4$-CH_2-CO_2), 79.1 (s, *C*$_5$Me$_4$-CH_2-CO_2), 34.6 (s, *C*H_2), 31.7 (m, *C*H_2), 29.2 (m, *C*H_2), 23.2 (m, *C*H_2), 19.3 (s, *C*H_2), 18.4 (s, *C*H_2), 16.6 (m, *C*H_2), 11.5 (s, *C*H_3), 11.2 (s, *C*H_3), −0.24 (s, Si-(*C*H_3)$_3$; FTIR (ATR, benzene film) ν: 1,716 cm^{-1} (C=O); HRMS–LIFDI (*m*/*z*): [M]$^+$ calcd for $C_{28}H_{55}FeO_2P_2ClSi$, 604.2485; found, 604.2474.

[(η^5–C_5Me_4–CH_2–$CO_2Si(CH_3)_3$)Fe(d*n*ppe)][BPh_4] (**3**; $C_{52}H_{72}FeO_2P_2SiB$, MW = 888.9 g/mol): In a glovebox, compound **2** (11.4 mg, 0.019 mmol) was dissolved in diethyl ether in a 20 mL scintillation vial. $NaBPh_4$ (6.1 mg, 0.018 mmol, 0.95 equiv) was added and the reaction mixture was stirred for 24 h. Volatiles were removed in vacuo, and the solids washed with pentane (3 × 2 mL), where the residue was then dissolved in THF, filtered through Celite® 545, and volatiles removed in vacuo to afford **3** as a yellow–beige solid (18.3 mg, >99%). ^{31}P{^{1}H} NMR (243 MHz, THF-H_8, 298 K) δ_P 71.8 ppm (br).

[(η^5–C_5Me_4–CH_2–$CO_2Si(CH_3)_3$)Fe(d*n*ppe)NCCD_3][BPh_4] (**4**; $C_{54}H_{78}FeNO_2P_2SiB$, MW = 929.9 g/mol): In a glovebox, compound **2** (10.6 mg, 0.018 mmol) was placed in a scintillation vial and dissolved in THF–d_8. $NaBPh_4$ (6 mg, 0.018 mmol) was then added, followed by the addition of approximately 5 µL of CD_3CN, which immediately generated an orange-colored solution. Upon standing for 12 h, compound **4** slowly converted to compound **5**, in which the TMS group had been removed to reveal a carboxylic acid. This transformation was supported by the appearance of a new ^{1}H NMR resonance at δ_H 11.1 ppm (RCO_2H), together with a new broadened ^{31}P NMR resonance at δ_P 77.42 ppm, slightly upfield of that observed for **4** (δ_P 77.43 ppm). ^{1}H NMR (400 MHz, THF-d_8, 298 K) δ_H 7.28 (m, 8H, o-C_6H_5 BPh_4^-), 6.85 (m, 8H, *m*-C_6H_5 BPh_4^-), 6.71 (m, 4H, *p*-C_6H_5 BPh_4^-), 2.98 (s, 2H, η^5-C_5Me_4-(CH_2)), 2.07 (m, 4H, overlapping CH_2 signals), 1.86 (m, 6H, overlapping CH_2 signals), 1.67 (s, 6H, η^5-C_5Me_4-(µ-CH_2)), 1.62 (s, 6H, η^5-C_5Me_4-(µ-CH_2)), 1.50 (m, 6H, overlapping CH_2 signals), 1.23 (m, 4H, overlapping CH_2 signals), 1.07 (m, 12H, P-CH_2-CH_2-CH_3), 0.23 (s, 9H, Si-(CH_3)$_3$); ^{31}P{^{1}H} NMR (162 MHz, THF-d_8, 298 K) δ_P 77.43 (s, **4**), 77.42 (br, **5**); ^{11}B{^{1}H} NMR (128 MHz, THF-d_8, 298 K) δ_B −6.5 ppm; HRMS–ESI(+) (*m*/*z*): [M − H]$^+$, [**5** − H]$^+$ calcd for $C_{25}H_{46}FeO_2P_2$, 496.2322; found, 496.2309; FTIR (ATR, acetonitrile film) ν: 2,243 cm^{-1} (C≡N).

Reduction chemistry to give **6**–H/Cl and **8**–H/Cl: In the glovebox, complex **2** (8.1 mg, 0.013 mmol) was added to a 20 mL scintillation vial and dissolved in 1 mL of C_6D_6. $HBCy_2$ (11.9 mg, 0.067 mmol) was then added and the reaction mixture was allowed to stir. Upon stirring overnight (12 h), the solution changed from purple to orange. The product mixture was dried in vacuo giving several reduced products as a yellow oil (>95% conversion of **2** based on ^{31}P{^{1}H} NMR spectroscopy). Due to similarity in polarity, these compounds were inseparable. Treatment of the crude reaction mixture with $NaBPh_4$ (4.2 mg, 0.0123 mmol) to possibly remove any {Fe–Cl} impurities by halide abstraction in Et_2O, followed by stirring overnight, afforded a brown solution. Removal of the solvent in vacuo, followed by washing of the resulting solid with pentane (3 × 2 mL) and filtration through Celite® 545, afforded an

orange–brown solution. Dissolution of this material in C_6D_6 resulted in minor amounts (<2 mg) of mostly two isomers having Cp*–$CH_2CH_2OBCy_2$ connectivity, one an Fe–H (**6**–H), and the other, an Fe–Cl (**6**–Cl). ^{1}H NMR (400 MHz, C_6D_6, 298 K, selected signals) δ_H 6.18 (t, $^3J_{H–H}$ = 5.0 Hz, 1H, Cp*–$CH_2CH(OBCy_2)_2$ **6**–H) [18], 5.43 (t, $^3J_{H–H}$ = 5.0 Hz, 1H, Cp*–$CH_2CH(OBCy_2)_2$ **6**–Cl), 4.01 (t, $^3J_{H–H}$ = 7.6 Hz, 2H, Cp*–$CH_2CH_2OBCy_2$ **8**–H) [18], 3.95 (t, $^3J_{H–H}$ = 7.6 Hz, 2H, Cp*–$CH_2CH_2OBCy_2$ **8**–Cl), 3.04 (d, $^3J_{H–H}$ = 5.0 Hz, 2H, Cp*–$CH_2CH(OBCy_2)_2$ **6**–H), 2.89 (d, $^3J_{H–H}$ = 5.0 Hz, 2H, Cp*–$CH_2CH(OBCy_2)_2$ **6**–Cl), 2.78 (t, $^3J_{H–H}$ = 7.6 Hz, 2H, Cp*–$CH_2CH_2OBCy_2$ **8**–H), 2.61 (t, $^3J_{H–H}$ = 7.6 Hz, 2H, Cp*–$CH_2CH_2OBCy_2$ **8**–Cl); $^{13}C\{^1H\}$ NMR (101 MHz, C_6D_6, 298 K, selected signals by ^{1}H,^{13}C HSQC) δ_C 94.42 (Cp*–$CH_2CH(OBCy_2)_2$ **6**–Cl), 94.06 (Cp*–$CH_2CH(OBCy_2)_2$ **6**–H), 65.8 (s; Cp*–CH_2CH_2–$OBCy_2$ **8**–H), 64.18 (s; Cp*–$CH_2CH_2OBCy_2$ **8**–Cl), 37.99 (Cp*–$CH_2CH(OBCy_2)_2$ **6**–Cl), 36.40 (Cp*–$CH_2CH(OBCy_2)_2$ **6**–H), 31.9 (s, Cp*–$CH_2CH_2OBCy_2$ **8**–H), 29.72 ppm (s, Cp*–$CH_2CH_2OBCy_2$ **8**–Cl); ^{11}B (128 MHz, C_6D_6, 298 K, selected signals) δ_B 45–55 ppm (br; $(RO)BCy_2$); $^{31}P\{^1H\}$ NMR (162 MHz, THF-d_8, 298 K) δ_P 97.8 (d, $J_{H,P}$ = 21.0 Hz, **6**–H), 79.0 (s, **6**–Cl); HRMS–LIFDI (*m*/*z*): $[M]^+$ calcd for **8**–H, $C_{37}H_{71}BFeOP_2$, 660.4423; found, 660.4416; $[M]^+$ calcd for **8**–Cl, $C_{37}H_{70}BClFeOP_2$, 694.4033; found, 694.4025; $[M]^+$ calcd for **6**–H, $C_{49}H_{92}B_2FeO_2P_2$, 852.6108; found, 852.6102.

Supporting Information

Spectroscopic data for all complexes. CCDC 2575113 contains the supplementary crystallographic data for this paper. These data can be obtained free of charge from The Cambridge Crystallographic Data Centre via https://www.ccdc.cam.ac.uk/data_request/cif.

Supporting Information File 1

Copies of spectra and crystallography details.
[https://www.beilstein-journals.org/bjoc/content/supplementary/1860-5397-22-104-S1.pdf]

Supporting Information File 2

Crystallographic information file (CIF) and checkCIF file.
[https://www.beilstein-journals.org/bjoc/content/supplementary/1860-5397-22-104-S2.zip]

Funding

M.W.D. is grateful to Western University, the Council of Ontario Universities for a John C. Polanyi award, the Canadian Foundation for Innovation (LOF–212442), and the Natural Sciences and Engineering Research Council of Canada (NSERC) for Discovery Grants, RGPIN–2020–04480/2026–06650, and Discovery Launch Supplement, DGECR–2020–00183 for funding. L.J.T. thanks NSERC for CGRS–M/D awards.

Author Contributions

Logan J. Taylor: formal analysis; investigation; writing – original draft; writing – review & editing. Marcus W. Drover: conceptualization; formal analysis; funding acquisition; investigation; project administration; supervision; visualization; writing – original draft; writing – review & editing.

ORCID® iDs

Marcus W. Drover - https://orcid.org/0000-0002-2186-1040

Data Availability Statement

All data that supports the findings of this study is available in the published article and/or the supporting information of this article.

References

1. Anwar, M. N.; Iftikhar, M.; Khush Bakhat, B.; Sohail, N. F.; Baqar, M.; Yasir, A.; Nizami, A. S. Sources of Carbon Dioxide and Environmental Issue. In *Sustainable Agriculture Reviews 37;* Asiri, A.; Lichtfouse, E., Eds.; Sustainable Agriculture Reviews, Vol. 37; Springer Nature: Cham, Switzerland, 2019; pp 13–36. doi:10.1007/978-3-030-29298-0_2
2. Le Quéré, C.; Raupach, M. R.; Canadell, J. G.; Marland, G.; Bopp, L.; Ciais, P.; Conway, T. J.; Doney, S. C.; Feely, R. A.; Foster, P.; Friedlingstein, P.; Gurney, K.; Houghton, R. A.; House, J. I.; Huntingford, C.; Levy, P. E.; Lomas, M. R.; Majkut, J.; Metzl, N.; Ometto, J. P.; Peters, G. P.; Prentice, I. C.; Randerson, J. T.; Running, S. W.; Sarmiento, J. L.; Schuster, U.; Sitch, S.; Takahashi, T.; Viovy, N.; Van Der Werf, G. R.; Woodward, F. I. *Nat. Geosci.* **2009,** *2,* 831–836. doi:10.1038/ngeo689
3. Revelle, R. *Sci. Am.* **1982,** *247,* 35–43. doi:10.1038/scientificamerican0882-35
4. Liu, C.; Cao, S.; Wei, Y.; Chen, Z.; Liu, S.; Chen, H.; Yin, Y.; Wei, S.; Wang, Z.; Lu, X. *J. Mater. Chem. A* **2025,** *13,* 8015–8023. doi:10.1039/d4ta08838g
5. Wang, Q.; Liu, K.; Fu, J.; Cai, C.; Li, H.; Long, Y.; Chen, S.; Liu, B.; Li, H.; Li, W.; Qiu, X.; Zhang, N.; Hu, J.; Pan, H.; Liu, M. *Angew. Chem., Int. Ed.* **2021,** *60,* 25241–25245. doi:10.1002/anie.202109329
6. Leonzio, G.; Hankin, A.; Shah, N. *Chem. Eng. Res. Des.* **2024,** *208,* 934–955. doi:10.1016/j.cherd.2024.07.014
7. Morimoto, T.; Nakajima, T.; Sawa, S.; Nakanishi, R.; Imori, D.; Ishitani, O. *J. Am. Chem. Soc.* **2013,** *135,* 16825–16828. doi:10.1021/ja409271s
8. Hueffel, J. A.; Rigoulet, M.; Wellig, S.; Sperger, T.; Ward, J. S.; Rissanen, K.; Schoenebeck, F. *J. Am. Chem. Soc.* **2025,** *147,* 26149–26157. doi:10.1021/jacs.5c00441
9. Grice, K. A. *Coord. Chem. Rev.* **2017,** *336,* 78–95. doi:10.1016/j.ccr.2017.01.007
10. Franco, F.; Rettenmaier, C.; Jeon, H. S.; Roldan Cuenya, B. *Chem. Soc. Rev.* **2020,** *49,* 6884–6946. doi:10.1039/d0cs00835d

11. Zhang, H.; Liang, Q.; Xie, K. *iScience* **2024,** *27,* 108973. doi:10.1016/j.isci.2024.108973
12. Liang, X.-M.; Ruan, Z.-J.; Guo, G.-Q.; Lin, J.-Q.; Zhong, D.-C. *ChemCatChem* **2025,** *17,* e202401394. doi:10.1002/cctc.202401394
13. Kostera, S.; Weber, S.; Blaha, I.; Peruzzini, M.; Kirchner, K.; Gonsalvi, L. *ACS Catal.* **2023,** *13,* 5236–5244. doi:10.1021/acscatal.3c00020
14. Kumar, A.; Gupta, R.; Mani, G. *Organometallics* **2026,** *45,* 410–423. doi:10.1021/acs.organomet.5c00354
15. Kostera, S.; Peruzzini, M.; Gonsalvi, L. *Catalysts* **2021,** *11,* 58. doi:10.3390/catal11010058
16. Das Neves Gomes, C.; Blondiaux, E.; Thuéry, P.; Cantat, T. *Chem. – Eur. J.* **2014,** *20,* 7098–7106. doi:10.1002/chem.201400349
17. Zurakowski, J. A.; Drover, M. W. *Chem. Commun.* **2023,** *59,* 11349–11352. doi:10.1039/d3cc03325b
18. Durfy, C. S.; Zurakowski, J. A.; Drover, M. W. *Angew. Chem., Int. Ed.* **2025,** *64,* e202580961. doi:10.1002/anie.202580961
19. Cramer, H. H.; Ye, S.; Neese, F.; Werlé, C.; Leitner, W. *JACS Au* **2021,** *1,* 2058–2069. doi:10.1021/jacsau.1c00350
20. Frogneux, X.; Jacquet, O.; Cantat, T. *Catal. Sci. Technol.* **2014,** *4,* 1529–1533. doi:10.1039/c4cy00130c
21. Scheuermann, M. L.; Semproni, S. P.; Pappas, I.; Chirik, P. J. *Inorg. Chem.* **2014,** *53,* 9463–9465. doi:10.1021/ic501901n
22. Niu, D.; Kostenko, A.; Kelly, J. A.; Sarkar, D.; Xu, H.; Inoue, S. *Chem. Sci.* **2025,** *16,* 4014–4022. doi:10.1039/d4sc07116f
23. Mazzotta, M. G.; Xiong, M.; Abu-Omar, M. M. *Organometallics* **2017,** *36,* 1688–1691. doi:10.1021/acs.organomet.7b00223
24. Pinkas, J.; Gyepes, R.; Polášek, M.; Mach, K.; Horáček, M. *Dalton Trans.* **2022,** *51,* 10198–10215. doi:10.1039/d2dt01344d
25. Zurakowski, J. A.; Brown, K. R.; Drover, M. W. *Inorg. Chem.* **2023,** *62,* 7053–7060. doi:10.1021/acs.inorgchem.3c00427
26. Allen, F. H.; Kirby, A. J. *J. Am. Chem. Soc.* **1984,** *106,* 6197–6200. doi:10.1021/ja00333a013
27. Hamon, P.; Toupet, L.; Roisnel, T.; Hamon, J.; Lapinte, C. *Eur. J. Inorg. Chem.* **2020,** 84–93. doi:10.1002/ejic.201901086
28. Zurakowski, J. A.; Durfy, C. S.; Stocek, N. B.; Fanchini, G.; Drover, M. W. *Chem. Sci.* **2024,** *15,* 10359–10365. doi:10.1039/d4sc03292f
29. Fulmer, G. R.; Miller, A. J. M.; Sherden, N. H.; Gottlieb, H. E.; Nudelman, A.; Stoltz, B. M.; Bercaw, J. E.; Goldberg, K. I. *Organometallics* **2010,** *29,* 2176–2179. doi:10.1021/om100106e
30. Tannenbaum, S.; Kaye, S.; Lewenz, G. F. *J. Am. Chem. Soc.* **1953,** *75,* 3753–3757. doi:10.1021/ja01111a043
31. Schmidbaur, H. *Chem. Ber.* **1964,** *97,* 1639–1648. doi:10.1002/cber.19640970617
32. Williams, D. B. G.; Lawton, M. *J. Org. Chem.* **2010,** *75,* 8351–8354. doi:10.1021/jo101589h

License and Terms

This is an open access article licensed under the terms of the Beilstein-Institut Open Access License Agreement (https://www.beilstein-journals.org/bjoc/terms), which is identical to the Creative Commons Attribution 4.0 International License (https://creativecommons.org/licenses/by/4.0). The reuse of material under this license requires that the author(s), source and license are credited. Third-party material in this article could be subject to other licenses (typically indicated in the credit line), and in this case, users are required to obtain permission from the license holder to reuse the material.

The definitive version of this article is the electronic one which can be found at:
https://doi.org/10.3762/bjoc.22.104

BEILSTEIN JOURNAL OF ORGANIC CHEMISTRY

Homogeneous copper-catalyzed aerobic oxidation of alcohols and aldehydes: mechanistic insights and recent advances

Hristo Petkov*[1] and Svilen P. Simeonov[1,2]

Review

Open Access

Address:
[1]Institute of Organic Chemistry with Centre of Phytochemistry, Bulgarian Academy of Sciences, Acad. G. Bonchev St., Bl. 9, 1113 Sofia, Bulgaria and [2]Research Institute for Medicines (iMed.ULisboa), Faculty of Pharmacy, Universidade de Lisboa, 1649-003 Lisbon, Portugal

Email:
Hristo Petkov* - hristo.petkov@orgchm.bas.bg

* Corresponding author

Keywords:
aerobic oxidation; alcohol oxidation; aldehyde oxidation; copper catalysis; mechanism

Beilstein J. Org. Chem. **2026,** *22,* 1323–1343.
https://doi.org/10.3762/bjoc.22.107

Received: 26 June 2026
Accepted: 09 September 2026
Published: 29 September 2026

This article is part of the thematic issue "Young investigators in earth-abundant metal catalysis".

Guest Editor: G. Lefevre

© 2026 Petkov and Simeonov; licensee Beilstein-Institut.
License and terms: see end of document.

Abstract

Copper-catalyzed aerobic oxidation of alcohols and aldehydes has become a key transformation for the sustainable synthesis of carbonyl compounds, combining high efficiency with the use of molecular oxygen as a benign terminal oxidant. Owing to its earth-abundance, low cost, low toxicity, and versatile redox properties, copper offers a compelling alternative to traditional noble metal catalysts and stoichiometric oxidation methods. This review highlights the evolution of copper-catalyzed aerobic oxidation of alcohols, emphasizing two distinct mechanistic regimes: nitroxyl radical-mediated systems and nitroxyl-free pathways, in which copper–ligand complexes directly promote dioxygen activation and substrate oxidation. Methods for conversion of aldehydes to carboxylic acids were also discussed. Apart from historical overview of the considered protocols, recent advances in the field were deliberated. Despite significant progress, the development of simpler, mediator-free catalytic systems based on readily available reagents remains a central challenge and a promising direction for future research.

Introduction

Carbonyl compounds, particularly aldehydes and ketones, are extremely valued commodities and building blocks in the pharmaceutical and chemical industries [1-9]. Beyond their use in traditional thermochemical synthesis, they have also found applications in modern fields like photochemistry [10] and electrochemistry [11]. These chemicals of higher oxidation state and importance are most often prepared via oxidation of alcohols [12]. Conventional oxidation methods in organic synthesis often use stoichiometric oxidants such as chromium reagents [13], permanganates [14], or hypervalent iodine reagents [15], as well as classical protocols such as Swern [16], Corey–Kim [17], Parikh–Doering [18] and Pinnick [19] oxidations. While these traditional approaches have proved historically essential and remain in use today, they typically generate significant amounts of waste and are no longer favored due to sustainability issues [20,21]. In the pursuit of greener protocols, strate-

gies such as catalytic Oppenauer-type [22] and organocatalytic solvent-free [23] oxidations have also been developed. Nevertheless, systems utilizing abundant first-row transition metals remain particularly attractive, among which copper plays a central role. Beyond copper chemistry, significant research efforts have also been devoted to the development of iron-catalyzed oxidations [24], yielding several robust, sustainable and widely recognized protocols [25-28].

Copper-catalyzed oxidation reactions offer a compelling and environmentally benign alternative to traditional methods, especially when molecular oxygen is employed as the terminal oxidant [29]. Copper has gained prominence due to its earth-abundance, low cost, and rich redox chemistry, and thus offers an appealing option from both economic and environmental perspectives [29,30]. In addition to these advantages, when compared to other transition metals, copper exhibits a remarkably lower toxicity profile. According to the ICH Q3D (R2) guidelines on elemental impurities [31], copper features a high oral permitted daily exposure (3400 µg/day), allowing residual concentrations of up to 340 ppm in final products, whereas much stricter limits apply to metals such as gold (32 ppm), nickel (22 ppm), palladium (10 ppm) and cobalt (5 ppm). Since traces of toxic metal impurities are often difficult to remove from the products, this regulatory advantage of copper significantly minimizes the costs and complexity associated with post-synthetic purification in the agrochemical and pharmaceutical industries.

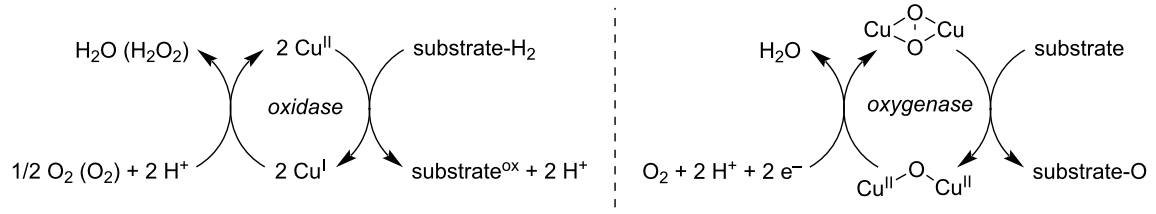
In recent decades, copper catalysis has evolved considerably, with the development of ligand-enabled variants that have opened new avenues for carbon–carbon and carbon–heteroatom-bond formation [32-34], as well as a broad range of oxidative transformations [35-37].

Among others, copper-catalyzed oxidation of alcohols to aldehydes or ketones, and of aldehydes to carboxylic acids, has been of central focus over the years [21,29]. These reactions are of fundamental importance for both laboratory and industrial chemistry, as they provide straightforward access to valuable chemicals. While several reviews have addressed related topics, many are now outdated or treat these transformations within broader contexts [21,29,36,38-43]. To address the lack of a focused and up-to-date overview specifically dedicated to these substrate classes, this review will discuss their relevant copper-catalyzed aerobic oxidation reactions.

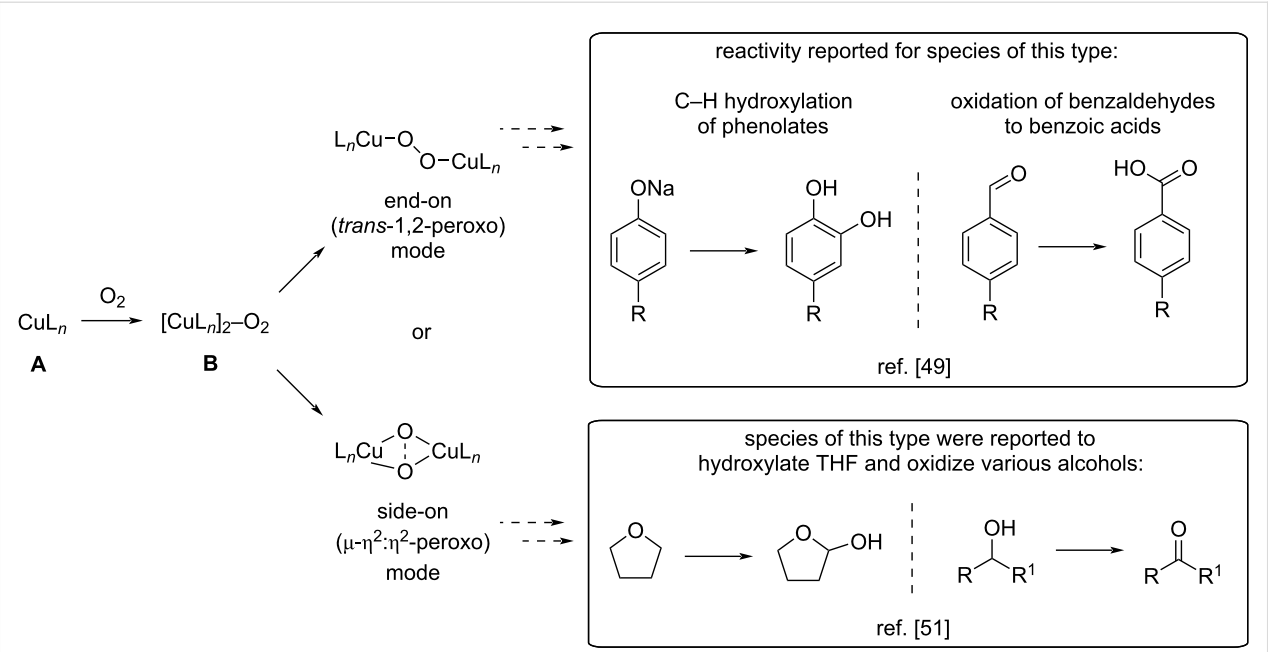
The use of oxygen is particularly appealing from a sustainability point of view, as it is inexpensive, readily available, and produces water as the only stoichiometric by-product in most instances [44]. These important features have driven extensive research into natural aerobic pathways and the creation of novel synthetic methodologies based on them. In all of these processes, oxygen functions either as an oxidant reduced to water (oxidase-like activity), a reactant embedded into the final product (oxygenase-like activity), or fulfills both roles simultaneously. In copper-based oxidations the oxidase catalytic cycle simply utilizes O_2 as a two-electron or two-proton acceptor in the catalytic oxidation of organic molecules. In the reaction, oxygen atoms are eventually reduced to either H_2O or H_2O_2. Thus the transfer of O atoms to the substrate is not observed. In the oxygenase catalytic cycle, the oxidation of substrate involves O transfer from O_2, often through a high-valent metal oxyl intermediate, while the other O atom is reduced to H_2O (Scheme 1) [45,46].

Dioxygen–dicopper complexes have been extensively investigated as key species in copper-mediated oxidation reactions [47]. Mechanistically, a Cu(I) complex **A** reacts with O_2 to generate a Cu_2–O_2 species **B**. The O_2-derived unit may adopt different coordination geometries depending on the ligand environment, including end-on (μ-1,2-) [48,49] or side-on (μ-η^2:η^2) [50,51]. Although several Cu/O_2 species can be formed during dioxygen activation by copper, and some of them can interconvert [52-54], two of the most well-studied Cu_2-O_2 complexes, bearing *trans*-1,2-peroxo or (μ-η^2:η^2-peroxo)dicopper cores, have been proposed as reactive intermediates that promote substrate oxidation (Scheme 2).

This review encompasses the important historical background and development of Cu-catalyzed aerobic oxidation of alcohols and aldehydes, as well as the most recent reports on the topic. It



Scheme 1: Oxidase- and oxygenase-like copper-based oxidation reactions.



Scheme 2: Formation and coordination modes (end-on vs side-on) of dioxygen–dicopper complexes and their synthetic applications in oxidation reactions.

also puts emphasis on the mechanistic details behind these processes. Cu-catalyzed aerobic oxidation reactions can be broadly categorized into two mechanistically distinct classes. The first type involves nitroxyl-radical-mediated systems, where a redox-active organic co-catalyst operates in synergy with copper to enable efficient oxidation. The second includes nitroxyl-radical-free systems, in which copper–ligand complexes mediate both substrate activation and dioxygen turnover in the absence of an external redox mediator. Despite sharing common catalytic elements, these two approaches differ in their operative mechanisms and catalytic roles of the individual components.

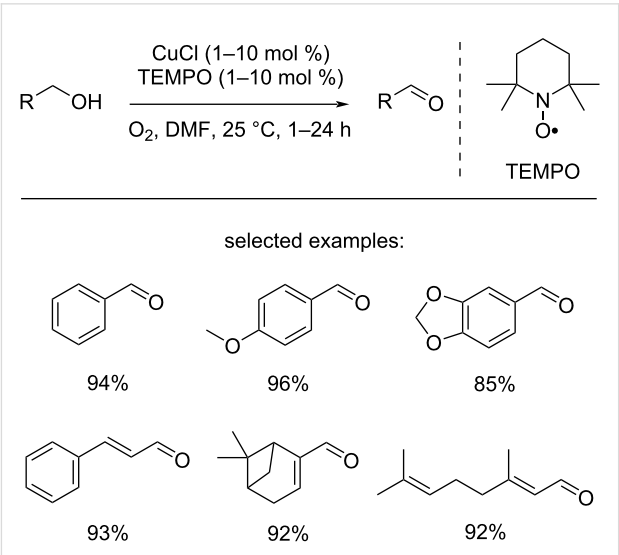
Review

Copper-catalyzed aerobic oxidation of alcohols to aldehydes and ketones

Nitroxyl radical-mediated Cu-catalyzed aerobic alcohol oxidation

The most widely used methods for aerobic alcohol oxidation rely on redox-active nitroxyl radicals in combination with Cu catalysts [42,46,55-57]. These radicals, especially when used together with the appropriate copper salt, have proven to be highly effective in selective and high-yielding aerobic alcohol oxidation reactions.

In 1984, Semmelhack et al. reported the first practical Cu-catalyzed aerobic oxidation of alcohols to aldehydes [58], using Cu in combination with the stable 2,2,6,6-tetramethyl-1-piperidine-*N*-oxyl radical (TEMPO) in DMF as a solvent at room temperature (Scheme 3). Although this system operated without a ligand and generally achieved excellent yields of around 90% with no over-oxidation to acids, it was efficient only for primary activated (benzylic and allylic) alcohols.



Scheme 3: The first practical Cu-catalyzed aerobic oxidation of alcohols employing TEMPO.

While the pioneering work by Semmelhack and co-workers originally identified TEMPO as the alcohol oxidant, with CuCl

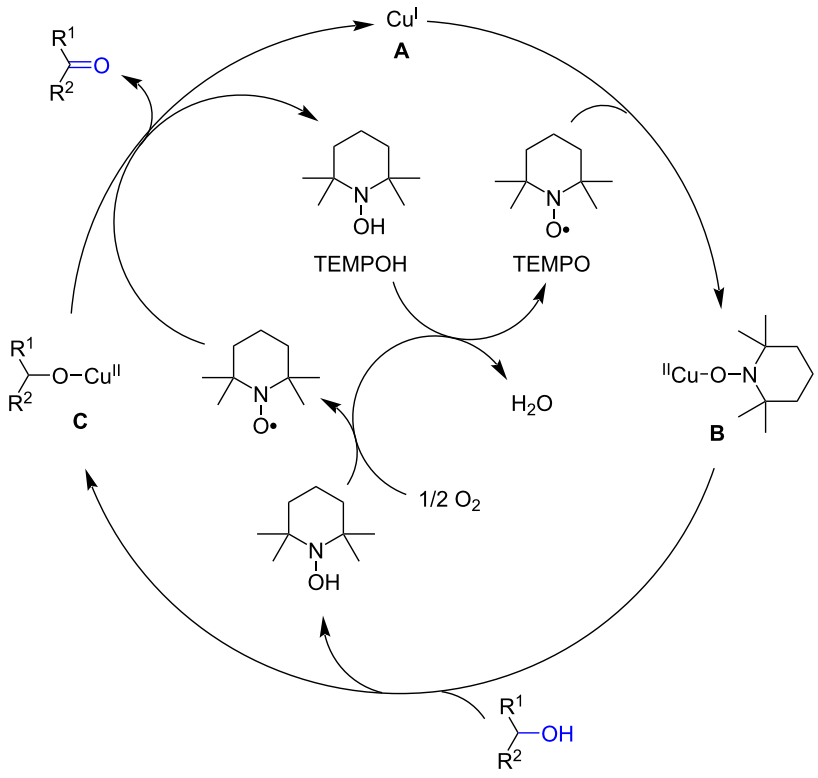
merely serving as a co-catalyst that drives TEMPO recycling, follow-up mechanistic investigations by Sheldon et al. [59] fundamentally revised this picture. Their findings revealed that Cu actually functions as the direct, substrate-selective redox catalyst, whereas TEMPO serves as the mediator responsible for regenerating the active copper species (as illustrated in Scheme 4).

As shown in the proposed catalytic pathway (Scheme 4), the initial step involves the interaction of copper(I) species **A** with TEMPO to yield the corresponding intermediate **B**. Subsequent reaction of **B** with the alcohol substrate generates copper(II) alkoxide complex **C** alongside TEMPOH (the reduced form of TEMPO). Complex **C** then reacts with another equivalent of TEMPO, furnishing the carbonyl product, an additional molecule of TEMPOH, and regenerating the copper(I) catalyst **A**. To close the cycle, the formed TEMPOH is re-oxidized to TEMPO in the presence of molecular oxygen (Scheme 4) [59,60].

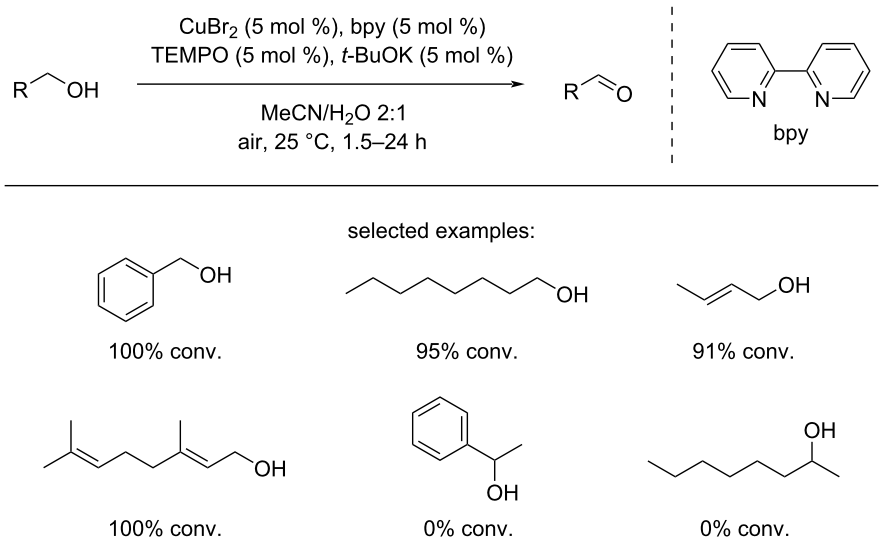
Furthermore, Sheldon and co-workers demonstrated that the combination of $CuBr_2$ and TEMPO, together with 2,2′-bipyridine (bpy) as a ligand, efficiently promotes the oxidation of primary alcohols to aldehydes without over-oxidation to acids [61]. A major feature of this remarkably mild protocol is its ability to deliver excellent conversions under ambient air (rather than pure oxygen) at room temperature. The method also exhibited excellent chemoselectivity as only primary alcohols were converted, in contrast to secondary alcohols' lack of reactivity (Scheme 5).

The complete lack of reactivity observed for secondary alcohols was attributed to sterics [61]. The presence of an additional R′ group in the secondary alcohols impairs the formation of species **A**, whereas its absence in primary alcohols allows for the stabilizing effect of the second β-hydrogen which facilitates the formation of radical species **B** (Figure 1).

In 2007, the group of Sekar [62] reported a method that utilizes CuCl, TEMPO, and 1,4-diazabicyclo[2.2.2]octane (DABCO), all in 5 mol %. The latter is suggested by the authors to serve a twofold purpose: deprotonating the alcohol's hydroxy group as a base and coordinating to CuCl as an N-donor ligand. Using nitromethane as a solvent under an oxygen atmosphere, various primary activated alcohols were smoothly transformed into the corresponding aldehydes at ambient conditions. Secondary alcohols, however, were found to be more challenging, requiring a high temperature (100 °C in toluene) and prolonged reaction time (Scheme 6). In addition, the catalytic system was



Scheme 4: Revisited mechanism of the Cu/TEMPO-catalyzed aerobic oxidation of alcohols by Sheldon et al. [59].



Scheme 5: $CuBr_2$/bpy/TEMPO-catalyzed oxidation of primary alcohols to aldehydes under air.

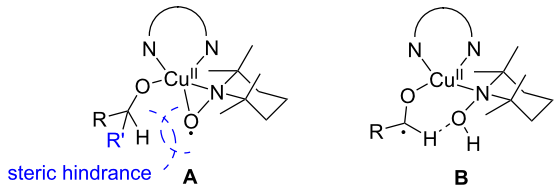
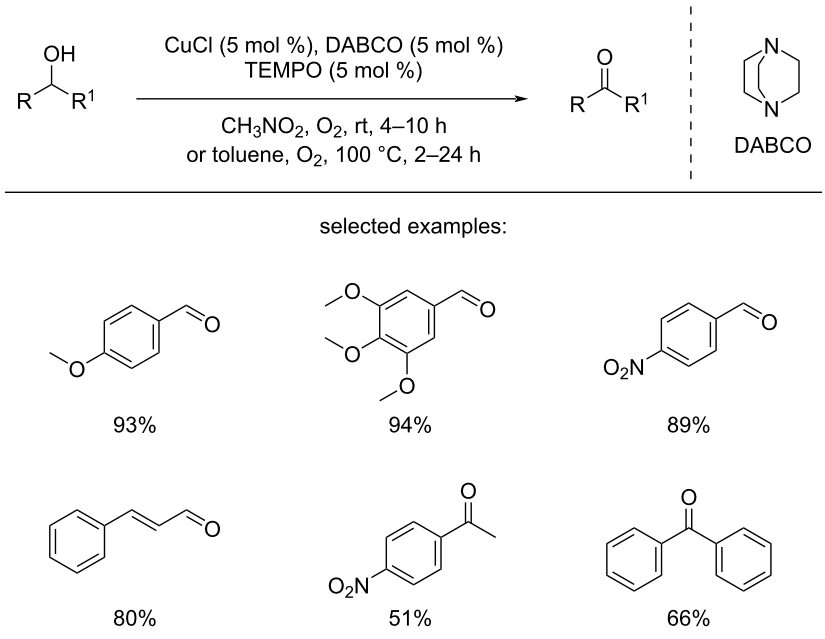


Figure 1: Possible explanation for the lack of reactivity of secondary alcohols proposed by Sheldon et al. [61].

proven insufficient for oxidizing aliphatic alcohols with satisfactory efficiency.

In 2011, an extensive study conducted by Hoover and Stahl discovered a new copper-based catalytic system (Cu/bpy/TEMPO/NMI) which showed a broad scope, excellent functional group tolerance, high efficiency towards oxidation of aliphatic substrates, and exquisite selectivity for primary alcohols [63]. Moreover, taking advantage of these features, the authors



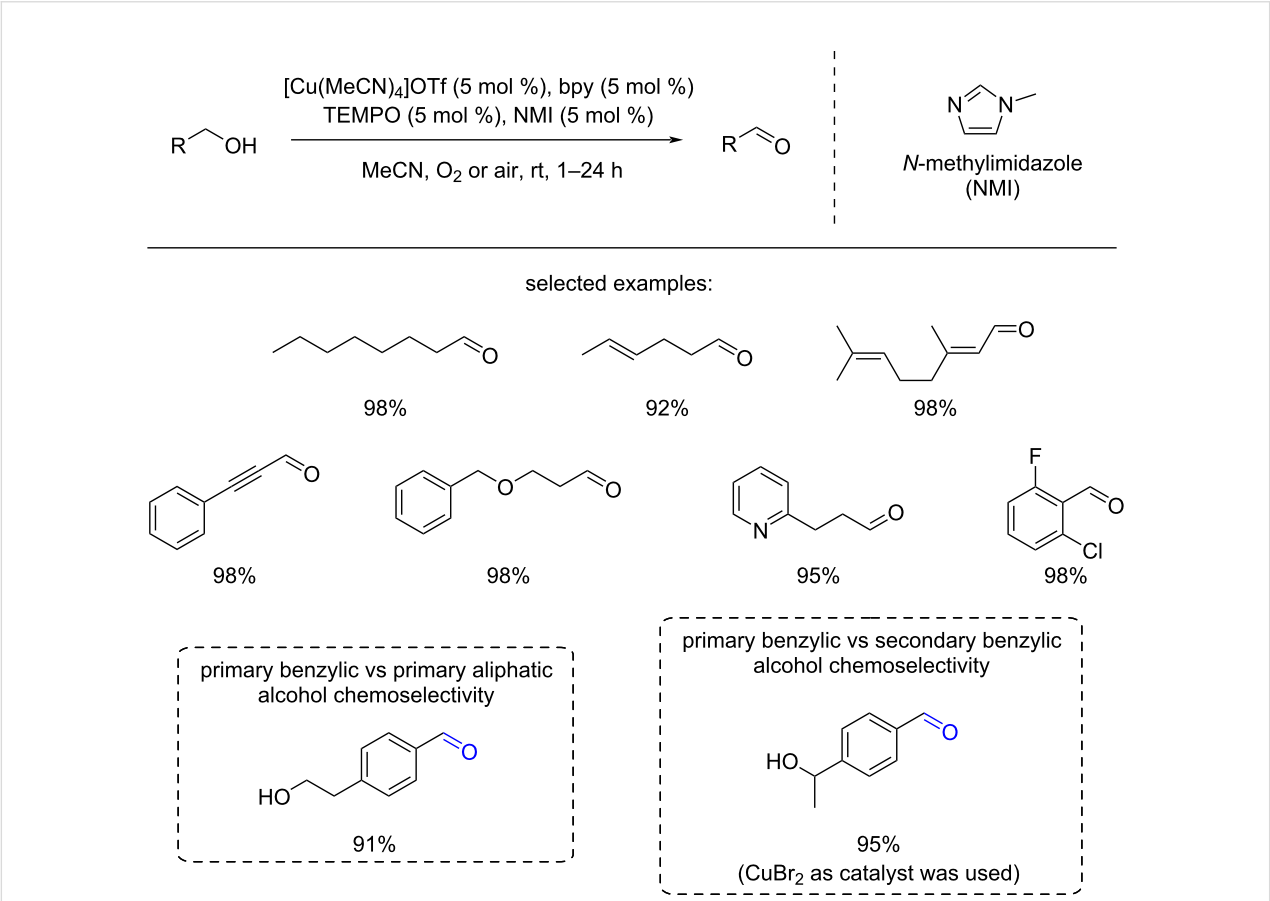
Scheme 6: The CuCl/DABCO/TEMPO system for the aerobic oxidation of activated alcohols.

achieved the selective oxidation of diols without the need of protecting groups (Scheme 7).

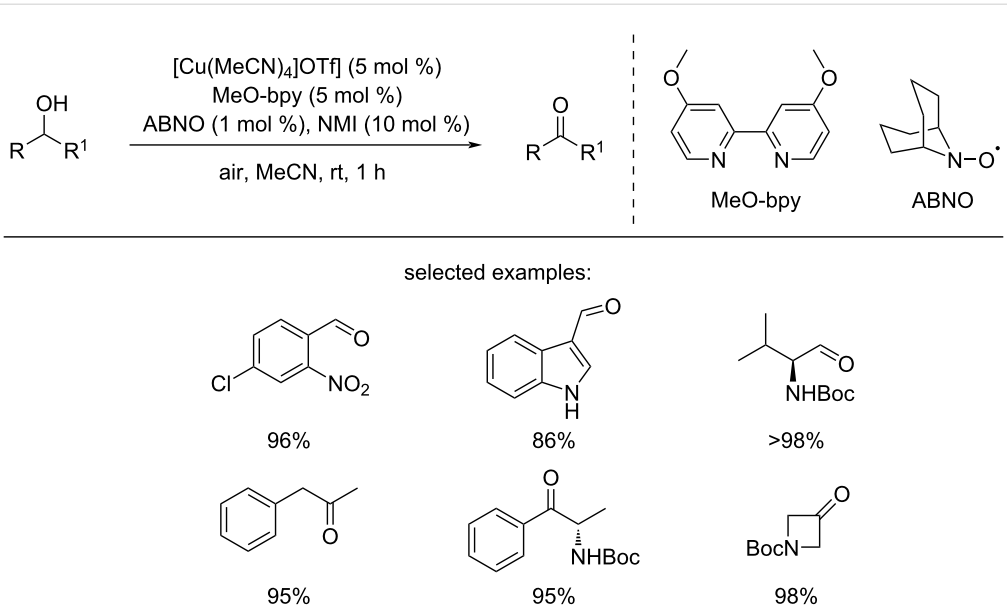
The insights from the method developed by Hoover and Stahl in 2011 [63] established a basis for overcoming the major limitation of the protocol, namely the non-reactivity of secondary alcohols. Although this method enables a highly chemoselective oxidation of primary alcohols over unprotected secondary ones, it comes at the expense of a narrower reaction scope. To overcome the limitations of their initial Cu/TEMPO system, in 2013, Steves and Stahl introduced a complementary catalytic system that employs the less sterically demanding nitroxyl radical 9-azabicyclo[3.3.1]nonane *N*-oxyl (ABNO) [64]. This refined approach exhibited exceptional catalytic activity across a broad range of substrates, smoothly converting primary as well as secondary alcohols, including benzylic, allylic, and aliphatic derivatives (Scheme 8). It is worth mentioning that although Stahl's TEMPO- and ABNO-based catalytic systems are comprised of several components, it was later discovered that their acetonitrile solutions offer long-term stability (≥1 year) when refrigerated and can be used directly in reactions, thereby improving operational simplicity of the protocols. In addition, these solutions have been made commercially available [65].

While the protocol reported by Stahl and Steves [64] was tested on several amino-functionalized molecules, in 2014, the group of Iwabuchi [66] disclosed a Cu/AZADO system (AZADO = 2-azaadamantane *N*-oxyl) for the oxidation of a broader spectrum of amino alcohols (Scheme 9). The authors found that the AZADO radical was superior to TEMPO and ABNO, and with AZADO loadings of 1–5 mol % a series of primary and secondary alcohols bearing either protected or unprotected amine functionalities were oxidized in good to excellent yields. Moreover, the method was further applied to the synthesis of the natural product (−)-mesembrine (Scheme 9).

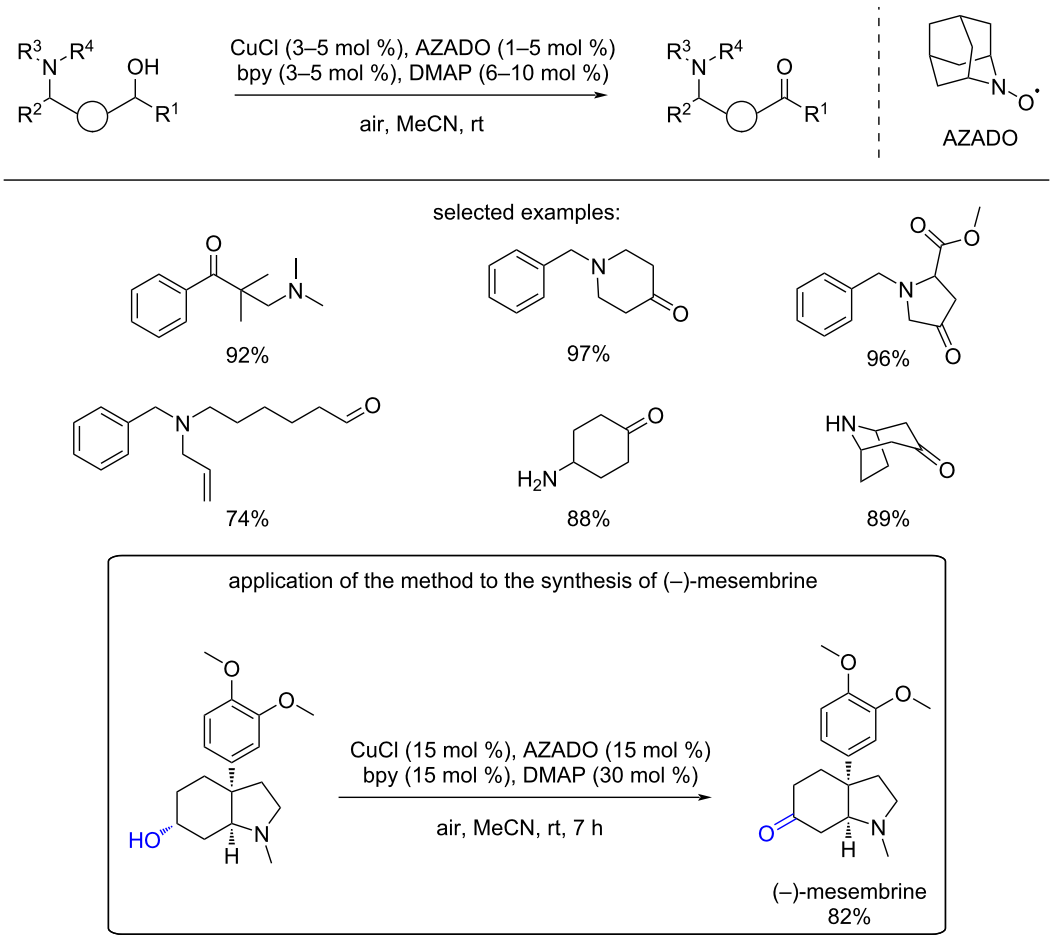
The group of Iwabuchi later extended the substrate scope of their catalytic system to oxidatively labile thioether-containing alcohols, including dithianes and sulfides [67]. Under optimized conditions, the chemoselective synthesis of the corresponding carbonyl products was achieved in good to high yields with preservation of the thioether groups (Scheme 10).



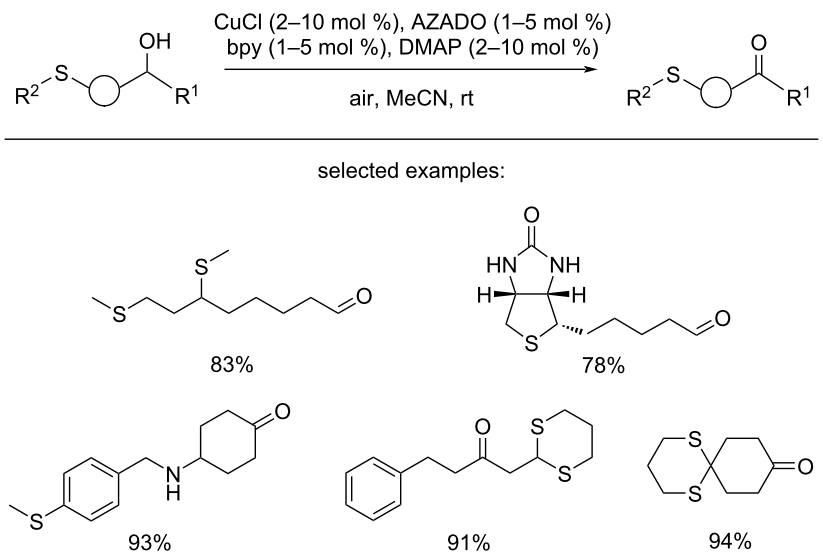
Scheme 7: The Cu/bpy/TEMPO/NMI system for the chemoselective aerobic oxidation of primary alcohols.



Scheme 8: The Cu/ABNO catalytic system for the aerobic oxidation of both primary and secondary alcohols.



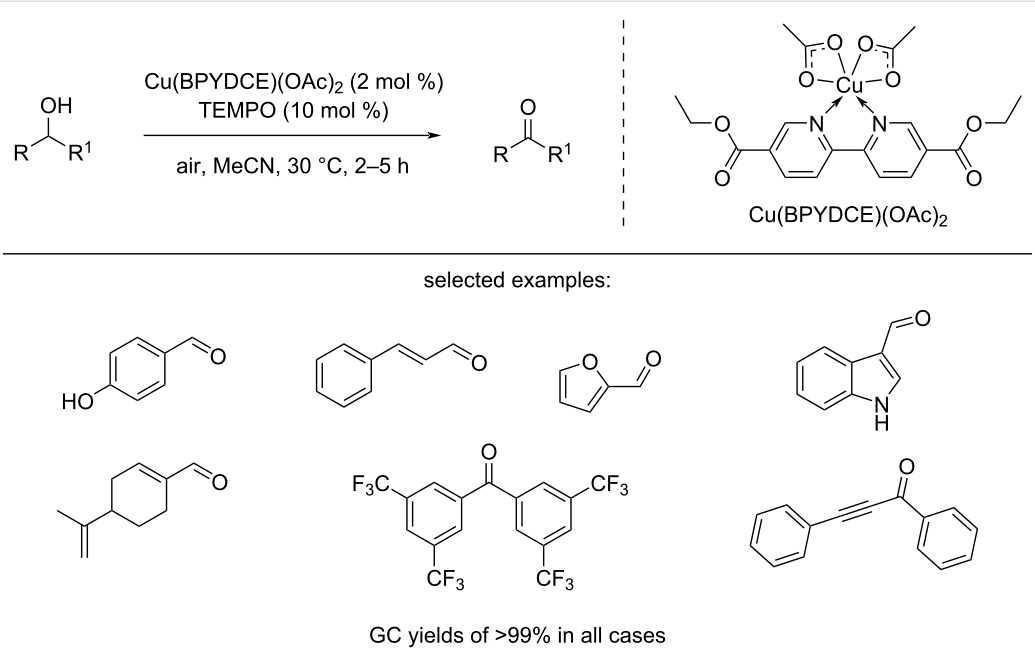
Scheme 9: The Cu/AZADO catalytic system for the aerobic oxidation of amino alcohols.



Scheme 10: The Cu/AZADO catalytic system for the aerobic oxidation of sulfur-containing alcohols.

The success of the described above nitroxyl-mediated oxidation relies on the presence of both ligand and a base. The need of additional base comes from the understanding that it assists the catalytic cycle through deprotonation of the alcohol, thus enhancing the substrate coordination to the Cu center. Moreover, it stabilizes the reactive catalytic species and accelerates molecular oxygen activation [40,41,68]. In an attempt to eliminate the need of external base, new catalytic systems have emerged in recent years.

For instance, TEMPO was successfully employed as a co-catalyst in a combination with $Cu(OAc)_2$/BPYDCDE complex (BPYDCDE = [2,2']bipyridinyl-5,5'-dicarboxylic acid diethyl ester) for the oxidation of both primary and secondary activated alcohols in the absence of exogenous base [69]. In all cases full conversions and analytical yields of >99% were achieved (based on GC analysis using *n*-decane as an internal standard), when the reactions were conducted under air at 30 °C in MeCN (Scheme 11).

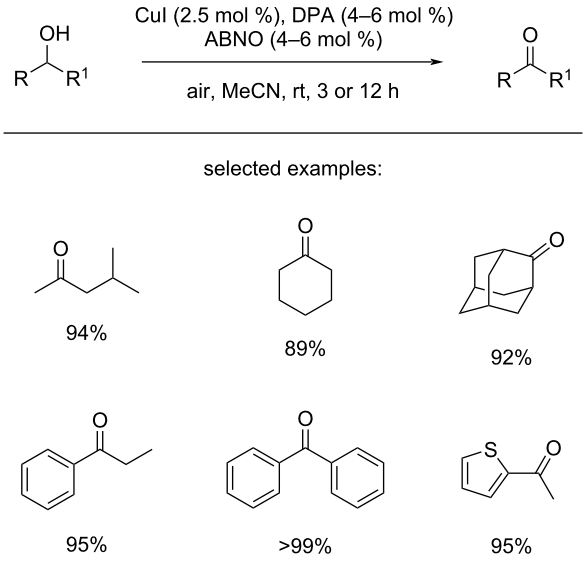


Scheme 11: $Cu(BPYDCE)(OAc)_2$/TEMPO-catalyzed external base-free aerobic oxidation of alcohols.

In 2022, the group of Repo [70] reported a base-free system comprised of the pre-catalyst CuI and 2,2′-dipyridylamine (DPA) acting as a ligand, along with TEMPO, that oxidizes primary aliphatic and benzylic alcohols at room temperature under air with nearly quantitative yields (Scheme 12). The authors also demonstrated the stability and applicability of their catalytic system under aqueous conditions.

In 2025, the same group reported a modified version, adapted for the oxidation of secondary alcohols [71]. By substituting TEMPO with ABNO, the authors expanded the substrate scope while employing the same DPA ligand (Scheme 13).

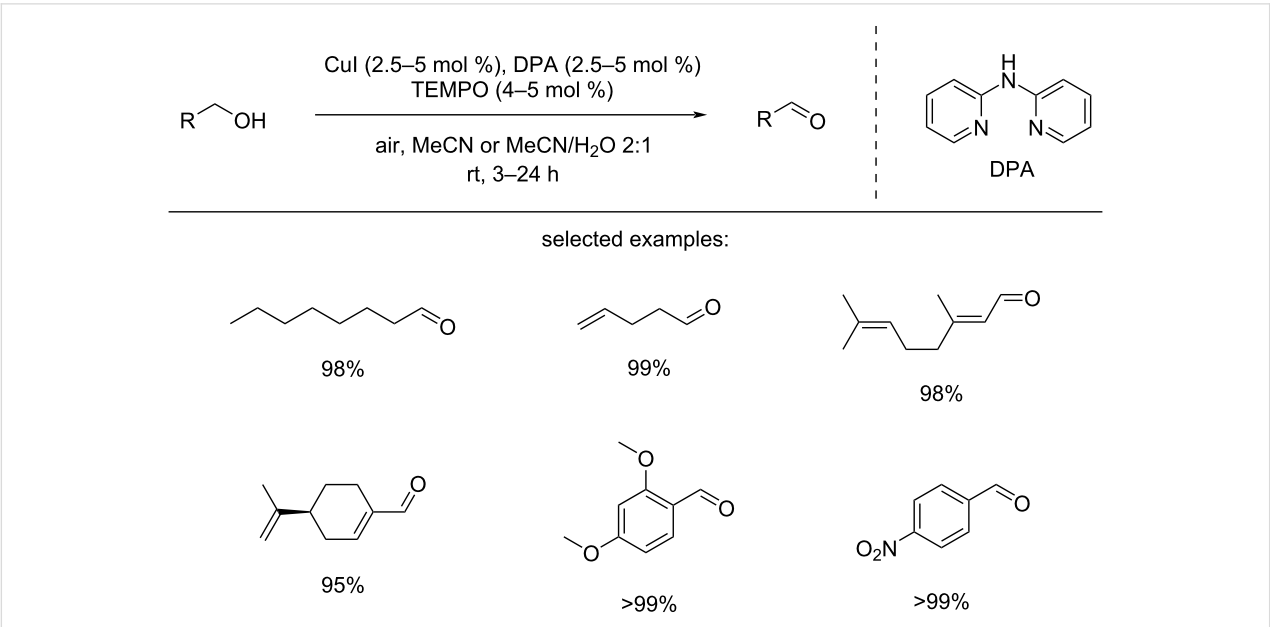
Zhai and Ma demonstrated that a Cu-catalyzed base- and ligand-free aerobic method can successfully oxidize a wide scope of allylic, propargylic, and benzylic alcohols, as well as allenols [72]. The process utilizes the cheap $Cu(NO_3)_2{\cdot}3H_2O$ salt coupled with TEMPO. Moreover, the authors showed the possibility of substituting TEMPO with the much cheaper 4-hydroxy-TEMPO (4-OH-TEMPO) while maintaining comparable outcome (Scheme 14).



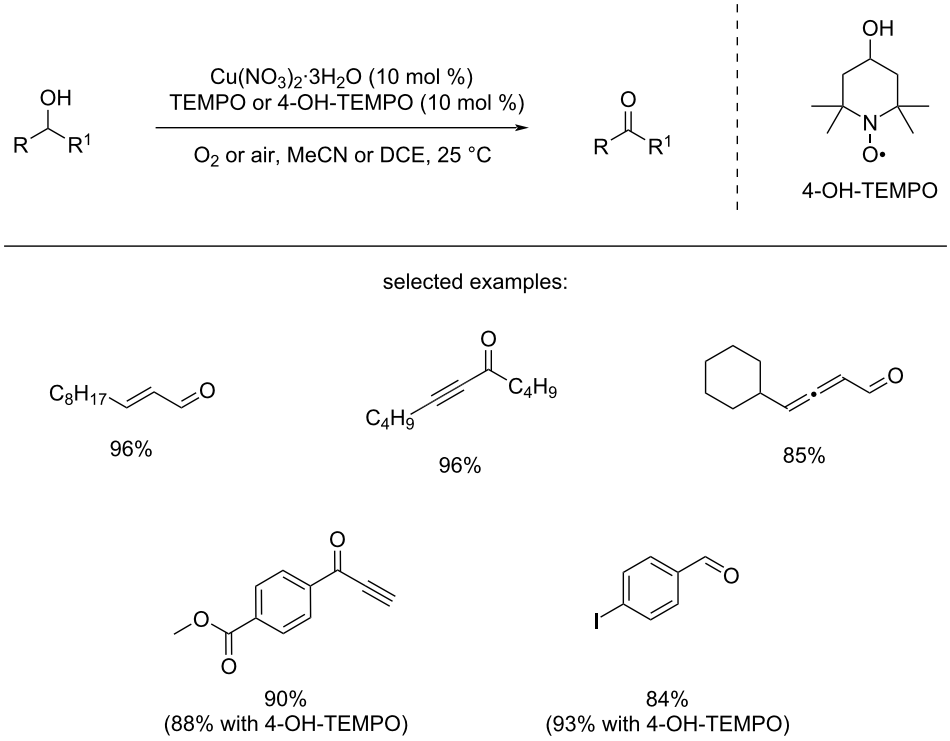
Scheme 13: Cu/DPA/ABNO base-free system for the oxidation of secondary alcohols.

Nitroxyl radical-free Cu-catalyzed aerobic alcohol oxidation

Early reports on nitroxyl radical-free Cu-mediated aerobic alcohol oxidation reactions focused on simple homogeneous complexes with nitrogenous ligands, such as pyridine, 2,2′-bipyridine, and 1,10-phenanthroline. These organic ligands primarily function as electron donors that stabilize various metal oxidation states while creating a steric environment at the metal center and thereby enhancing catalytic activity and selectivity. However, these early methods suffered from limited substrate scope since only activated benzylic and allylic alcohols could provide the corresponding aldehydes or ketones with satisfactory efficiency, whereas aliphatic alcohols proved incompatible. In several instances they were unreactive or underwent side reactions such as competing C–C-bond cleavage or over-oxidation to carboxylic acids [73-76]. Despite the common drawbacks, these preceding works have paved the way



Scheme 12: Cu/DPA/TEMPO base-free system for the oxidation of primary alcohols.



Scheme 14: Base- and ligand-free Cu-catalyzed aerobic oxidation of alcohols.

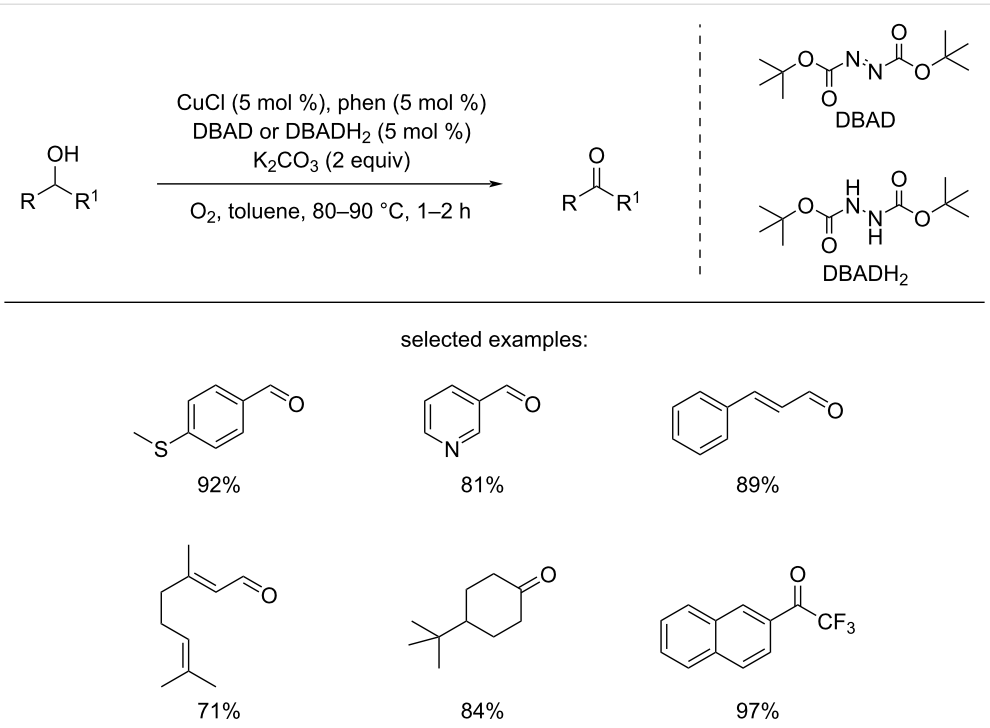
for more in-depth research in the field and later catalytic aerobic oxidations based on copper that do not rely on nitroxyl radicals have emerged. These protocols have brought improvements in terms of substrate scope, selectivity, and conversion.

Markó and co-workers pioneered much of the copper-catalyst development between the end of the 20th and the beginning of the 21st century. In their initial report in 1996, a combination of CuCl, 1,10-phenanthroline, and di-*tert*-butyl azodicarboxylate (DBAD) or di-*tert*-butyl hydrazodicarboxylate ($DBADH_2$), allowed the oxidation of alcohols with great functional group tolerance [77]. The method was applicable to a wide range of primary, secondary, allylic, and benzylic alcohols which were smoothly oxidized to the corresponding aldehydes or ketones with yields ranging from 71 to 97% (Scheme 15).

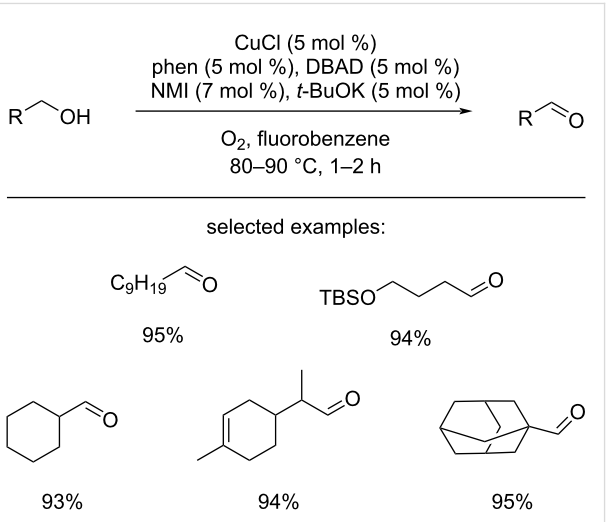
However, this system required the presence of 2 equivalents of a base (K_2CO_3) and was not consistent for the oxidation of primary aliphatic alcohols. To address this limitation, the same group [78] later improved the previously established protocol. They have found that a change of the solvent from toluene to fluorobenzene allowed the use of a catalytic amount of base (*t*-BuOK in 5 mol %). The addition of *N*-methylimidazole (7 mol %) further boosted the efficiency of the system ensuring high conversion of various primary aliphatic alcohols (Scheme 16).

The mechanism of the reaction proposed by Markó et al. is shown in Scheme 17A. The catalytic cycle initiates via a ligand exchange between Cu(I) phenanthroline hydroxide complex **A** and the alcohol substrate to yield the corresponding alkoxy species **B**. Subsequent alcohol oxidation to the target carbonyl compound proceeds concomitantly with diazodicarboxylate reduction to a hydrazide complex, followed by aldehyde dissociation that yields Cu(I) complex **C**. Aerobic oxidation of **C** then generates Cu(II) μ-peroxo species **D**. Finally, a homolytic peroxide bond (O–O) cleavage, which occurs with reduction of the copper center and oxidation of the hydrazide, restores the active Cu(I) catalyst **A** (Scheme 17A) [29,77,79]. Almost 20 years later, McCann and Stahl [80] conducted a detailed mechanistic study and further elucidated the mechanism which was initially proposed by Markó et al. [79]. They revealed that the reaction is driven by two interconnected catalytic cycles operating in succession. It begins with a rapid Cu/DBAD-mediated step where DBAD acts as the oxidant, followed by a slower, rate-limiting Cu-only pathway (Scheme 17B).

A method, initially described as nitroxyl radical-free, for Cu-catalyzed aerobic oxidation of alcohols was published by the groups of Arndtsen and Lumb in 2015 [81]. The approach utilizes $[Cu(MeCN)_4]PF_6$, *N*,*N*'-di-*tert*-butylethylenediamine (DBED) as a ligand and 4-dimethylaminopyridine (DMAP) as a base. A variety of activated as well as non-activated substrates



Scheme 15: Oxidation of alcohols catalyzed by Cu/phen/DBADH$_2$.



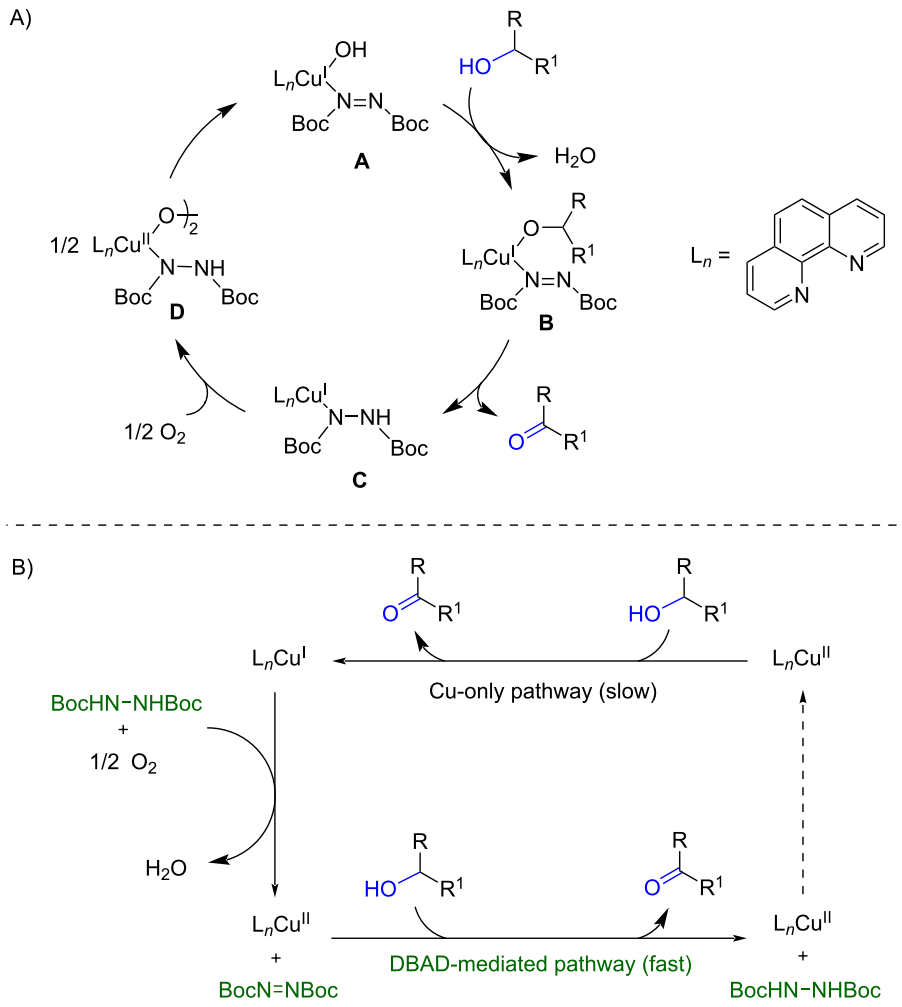
Scheme 16: Improved protocol for primary aliphatic alcohol oxidation by Markó et al. [78].

were well tolerated. The authors proved that the developed Cu/DBED-catalyzed oxidation offers important complementary selectivity to TEMPO-based systems, and favors the oxidation of activated secondary over primary alcohols (Scheme 18).

Two years later, however, a mechanistic study performed by the groups of Arndtsen and Stahl [82] challenged the initial claim that the method proceeds in the absence of nitroxyl radicals. The authors proved such species can, in fact, be generated in situ under the reaction conditions. Influenced by the Cu catalyst and oxygen atmosphere, the ligand, DBED, undergoes N-hydroxylation leading to the formation of a nitroxyl-type species (Scheme 19) which subsequently acts as a hydrogen atom abstractor – a role analogous to that of TEMPO in related oxidation systems.

Jiang et al. reported a mild Cu/NHC-catalyzed (NHC = N-heterocyclic carbene) aerobic oxidation of benzylic and heteroaromatic alcohols [83]. The method utilizes the commercially available NHC complex (SIPr)CuCl. In the presence of molecular sieves both primary and secondary alcohols were converted to the corresponding carbonyl products with high isolated yields (Scheme 20). However, beyond the requirement of two equivalents of a base (KOH), a major drawback of this protocol is its failure to oxidize aliphatic substrates. Despite these disadvantages, the authors highlighted the practicality of the protocol and achieved the synthesis of valuable imines and amines in a cascade one-pot fashion.

Z. Zhang and F. Zhang et al. introduced another nitroxyl radical-free approach for alcohol oxidation [84]. Their method implements a Cu catalyst featuring a redox-active ligand under an atmosphere of oxygen, without the need for a base additive. As shown in Scheme 21, a range of primary, secondary, aromatic, and aliphatic alcohols were smoothly oxidized at ambient



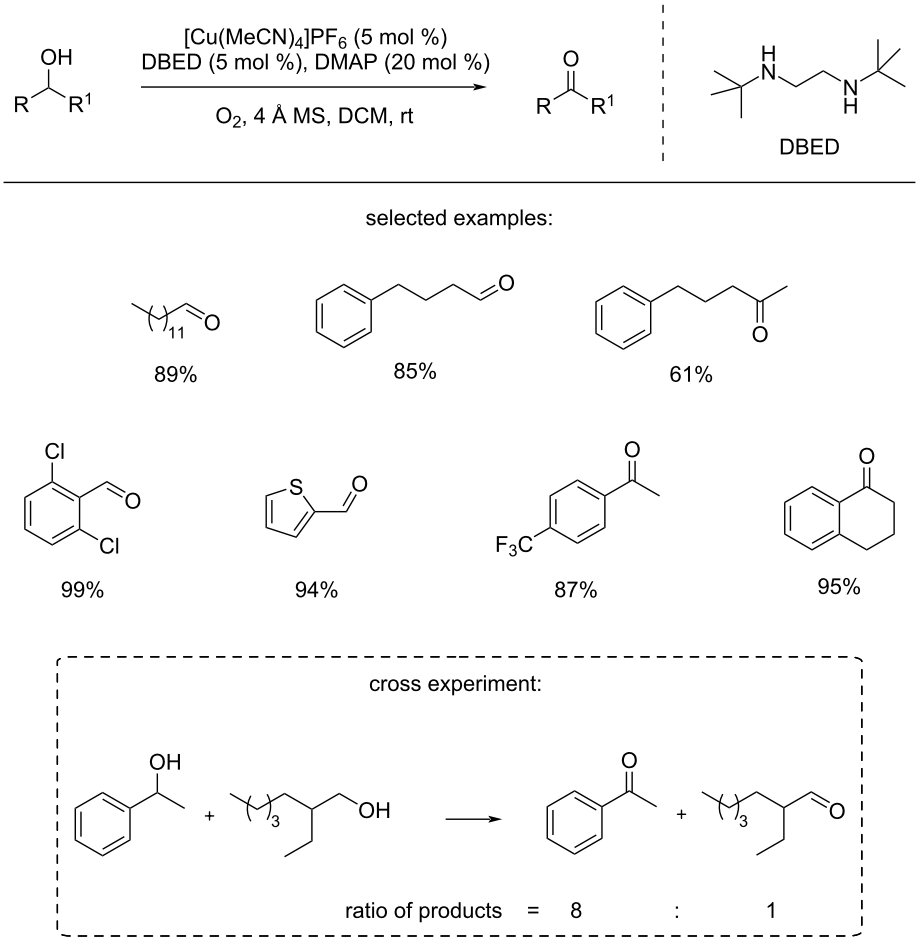
Scheme 17: Mechanism of the Cu/DBAD-catalyzed oxidation: A) initial proposal by Markó et al.; B) further elucidation by McCann and Stahl.

temperature in hexafluoroisopropanol (HFIP). The Cu catalyst, however, is not an off-the-shelf material and must be prepared ex situ via a two-step procedure prior to the catalytic reaction. Despite this drawback, the authors successfully adapted the protocol to continuous-flow conditions, which significantly enhanced the reaction rate and reduced the reaction duration from 24 hours (for the batch conditions) to just 40 min.

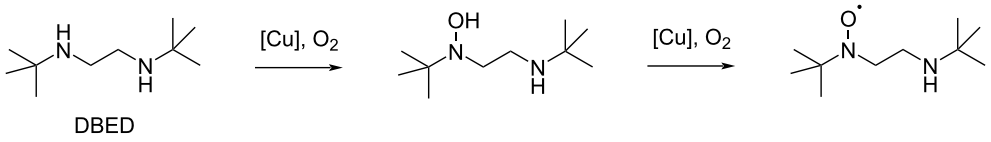
The utility and scalability of Cu-catalyzed aerobic oxidations have also attracted interest for pilot- and industrial-scale applications. Demonstrations of such protocols include process-intensified setups [85,86], as well as patented upscale methodologies for oxidations of primary and secondary alcohols [87,88]. Furthermore, the value of copper-catalyzed aerobic oxidation is increasingly amplified by the growing availability of biosourced alcohols derived from renewable biomass. Converting bio-derived chemicals such as 5-hydroxymethylfurfural [89-91] and various α-ketoalcohols [92,93] into high-value products under mild Cu-catalyzed conditions represents a key pillar of sustainable organic synthesis.

Copper-catalyzed aerobic oxidation of aldehydes to carboxylic acids

Copper-catalyzed aerobic oxidation has been further developed to promote not only the oxidation of alcohols to aldehydes but also the conversion of the latter into the corresponding carboxylic acids. While many catalytic systems are designed to achieve selective oxidation of alcohols and typically stop at the aldehyde stage, a number of methodologies have been reported that enable complete oxidation. The vast majority of existing protocols require the presence of water in the reaction mixture to establish an equilibrium between the aldehyde and its corresponding hydrate (*gem*-diol), as the latter serves as the actual intermediate undergoing oxidation to the desired acid. In such systems, aldehydes can be efficiently transformed into the corresponding carboxylic acids, and in certain cases, alcohols



Scheme 18: TEMPO-free Cu-catalyzed aerobic oxidation of alcohols reported by Arndtsen and Lumb [81].

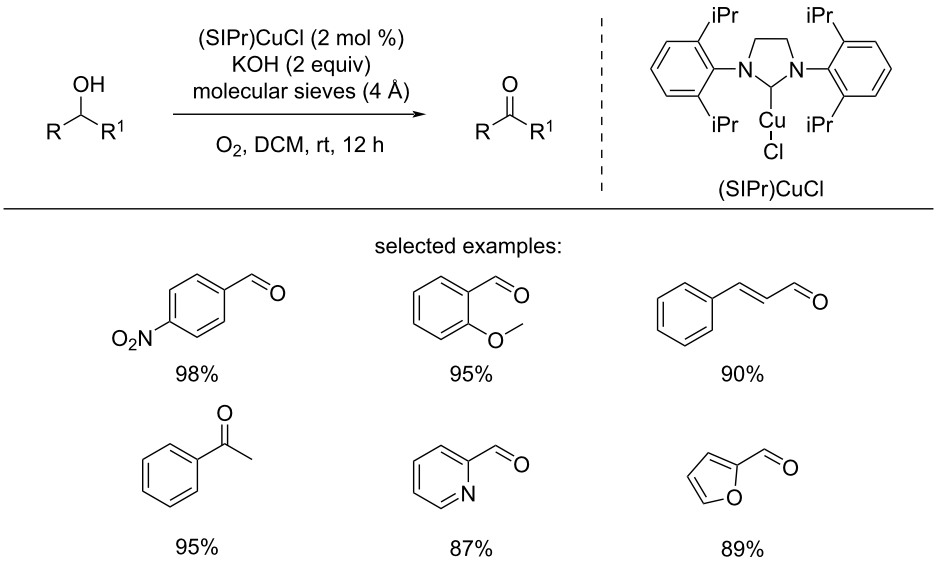


Scheme 19: In situ generation of *N*-oxyl radicals from DBED.

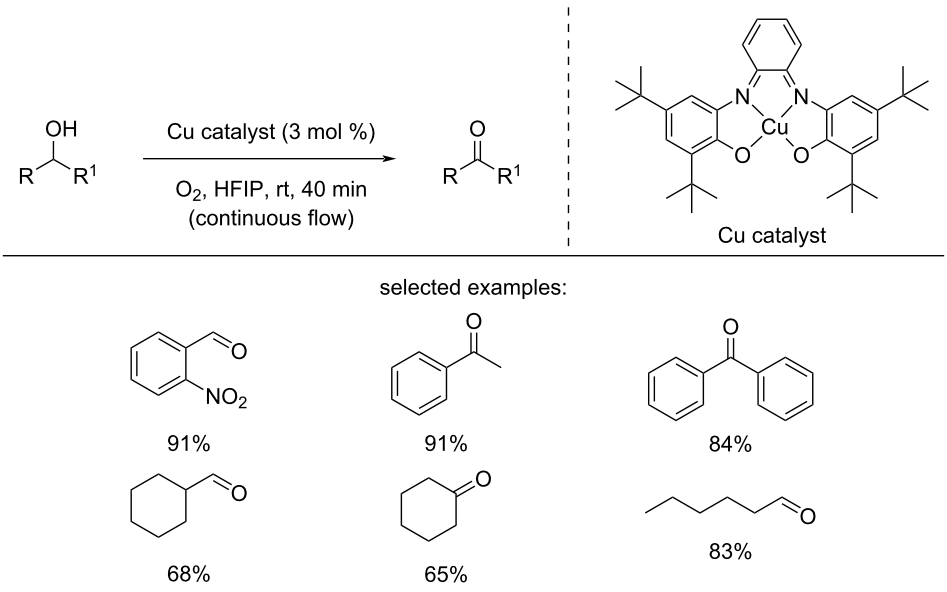
can be directly converted into acids in a one-pot fashion (Scheme 22) [94], which is particularly attractive from both the synthetic and the green chemistry standpoint.

Over the past decades, significant efforts have been directed toward the development of transition-metal-catalyzed aerobic oxidation of aldehydes to carboxylic acids, with early methodologies largely based on noble metal catalysts, e.g., palladium (Pd) [95], platinum (Pt) [95], gold (Au) [96], silver (Ag) [97], etc. Nonetheless, the cost and scarcity of precious metals limit their practicality. Therefore, exploring earth-abundant metals, such as Cu, is of significant importance.

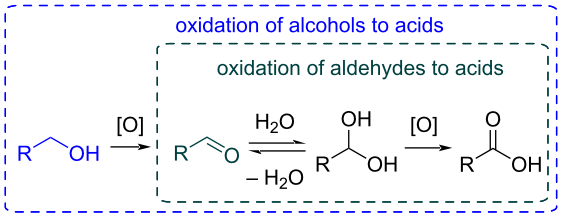
In 2016, the first example of homogeneous copper-catalyzed aerobic oxidation of aldehydes was presented [98]. The method utilizes a Cu/NHC system, namely $[Cu(acac)_2]$/SIMesCuCl, under atmospheric oxygen. The reported reaction proceeds under mild aqueous conditions, and covers a wide range of functionalized aldehydes (Scheme 23). Another advantage of this approach is that chromatography is generally not necessary for product purification. However, stoichiometric amount of a base (NaOH) is required. Identified by the authors as a catalytic Fehling's reaction, the proposed mechanism (depicted in Scheme 23) begins with the hydroxide-mediated conversion of NHC complex SIMesCuCl (**A**) into the



Scheme 20: (SIPr)CuCl-catalyzed aerobic oxidation of alcohols.

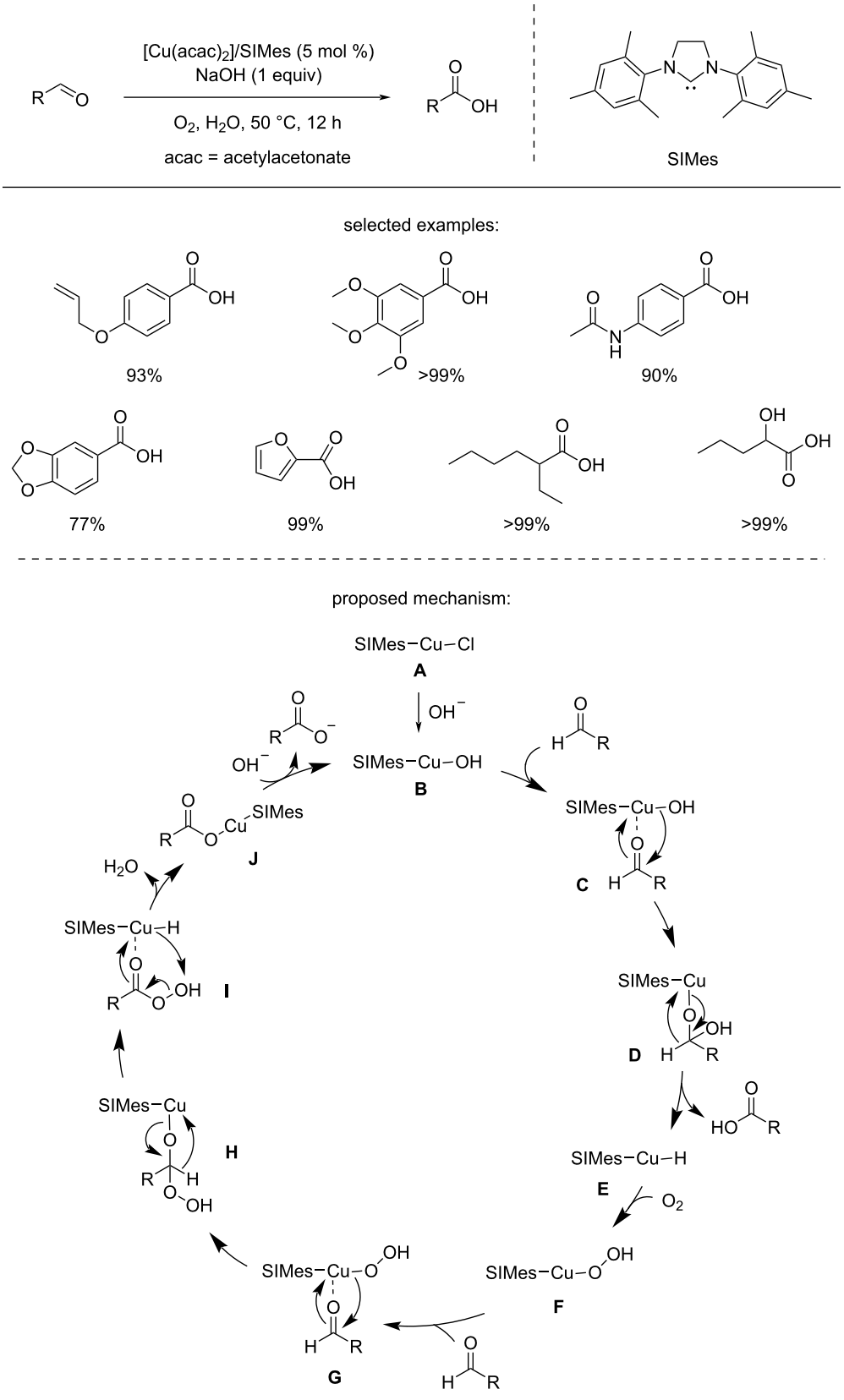


Scheme 21: Base- and nitroxyl radical-free Cu-catalyzed aerobic oxidation of alcohols under continuous-flow conditions.



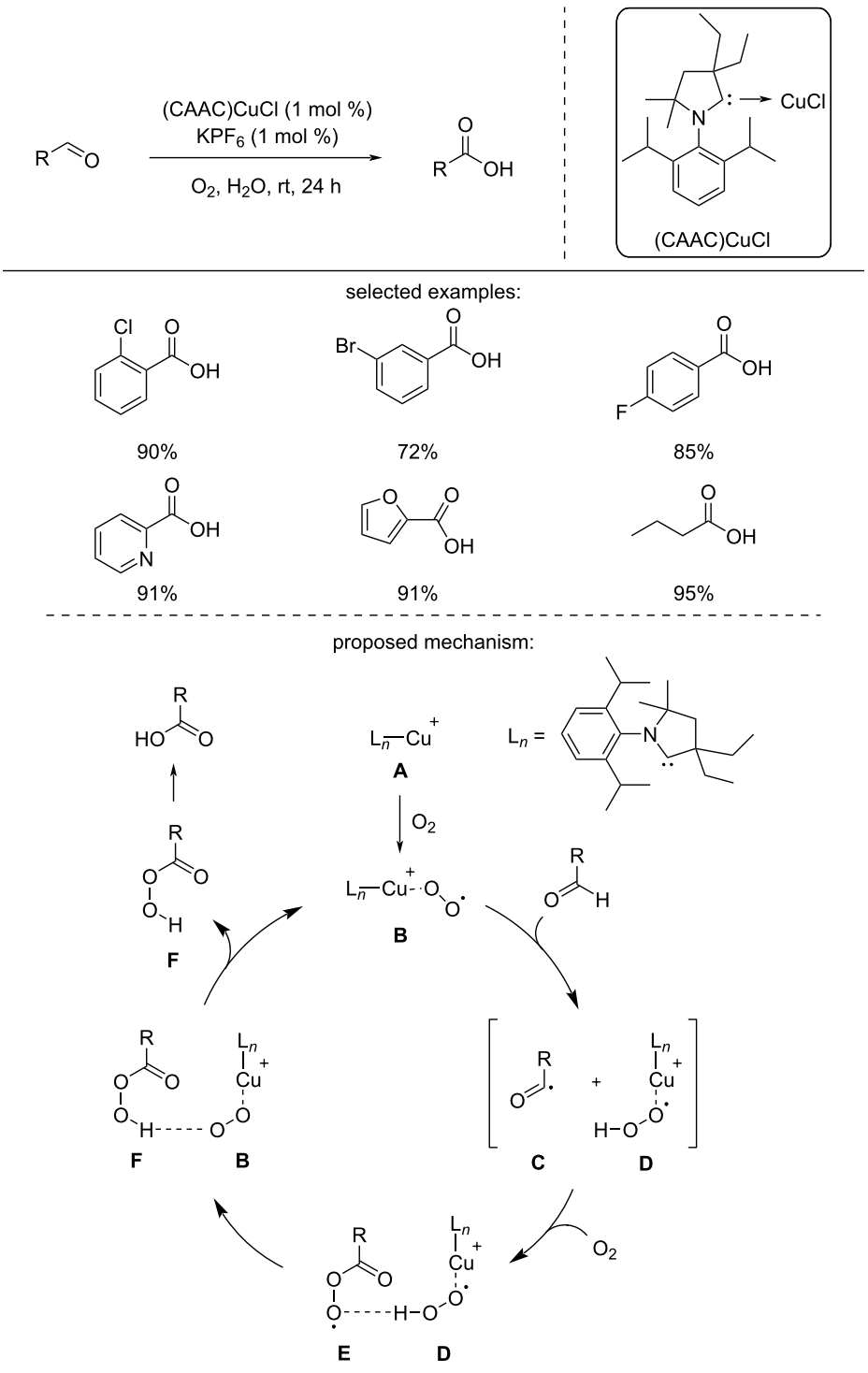
Scheme 22: Carboxylic acids as products of aldehyde and alcohol oxidations – general mechanism.

active SIMesCuOH (**B**). Aldehyde coordination to **B** generates **C**, which is attacked by a hydroxide ion to yield intermediate **D**. Subsequent β-hydride elimination affords the hydride **E**. Reaction of **E** with molecular oxygen affords hydroperoxide **F**, which coordinates a second aldehyde to form **G**. Attack of the hydroperoxide in **G** produces intermediate **H**, which undergoes hydride abstraction to form **I**. An intramolecular hydride-mediated peroxide reduction within **I** furnishes the carboxylate complex **J**. The catalytic cycle closes upon hydroxide substitution of the carboxylate, releasing the product and regenerating **B** [98].



Scheme 23: The first homogeneous Cu-catalyzed aerobic oxidation of aldehydes.

In 2022, a similar to the NHC-based copper catalysts, namely cyclic (alkyl)(amino)carbene copper chloride ((CAAC)CuCl) was reported to promote the aerobic oxidation of aldehydes (Scheme 24) [99]. The method operates at room temperature in water and uses only a catalytic amount of an additive (1 mol % of KPF_6) which is necessary for the release of the active cation **A**. The authors' mechanistic proposal is shown in Scheme 24. Upon generation of **A**, activation of molecular oxygen produces



Scheme 24: (CAAC)CuCl-catalyzed aerobic oxidation of aldehydes.

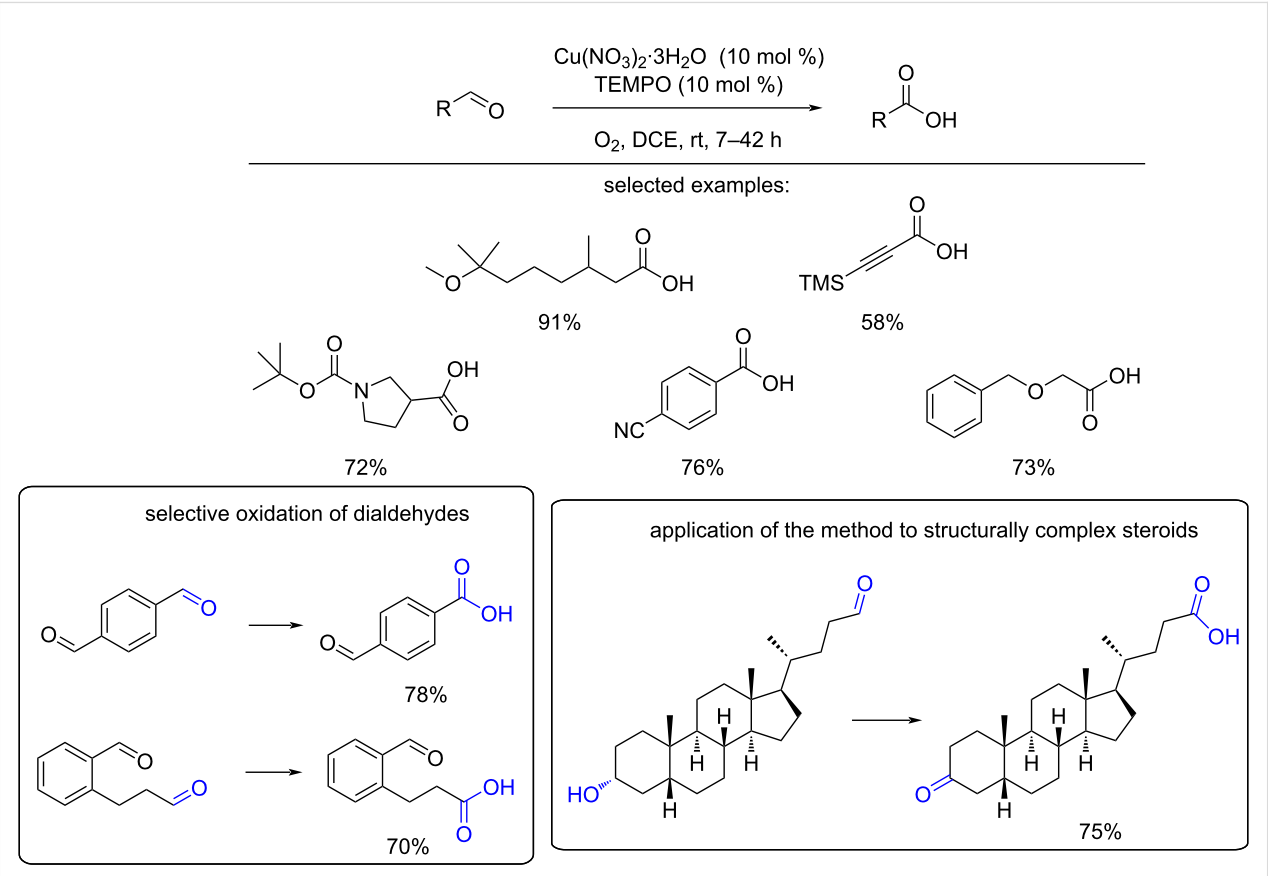
species **B**, which then abstracts the aldehyde's formyl hydrogen atom to form radical species **C** and **D**. In the presence of O_2, an acyl peroxy radical **E** is generated, which in turn re-abstracts the hydrogen of species **D** yielding peroxy acid **F**, and the cycle closes with the regeneration of species **B**. Due to the unstable nature of **F** under aqueous conditions, the final carboxylic acid product is formed [99].

The above-mentioned methods, however, share a major drawback – the catalyst (a complex between a copper salt and a carbene ligand) must be prepared ex situ in advance, which complicates the overall synthetic procedure by requiring additional preparation steps prior to the catalytic reaction.

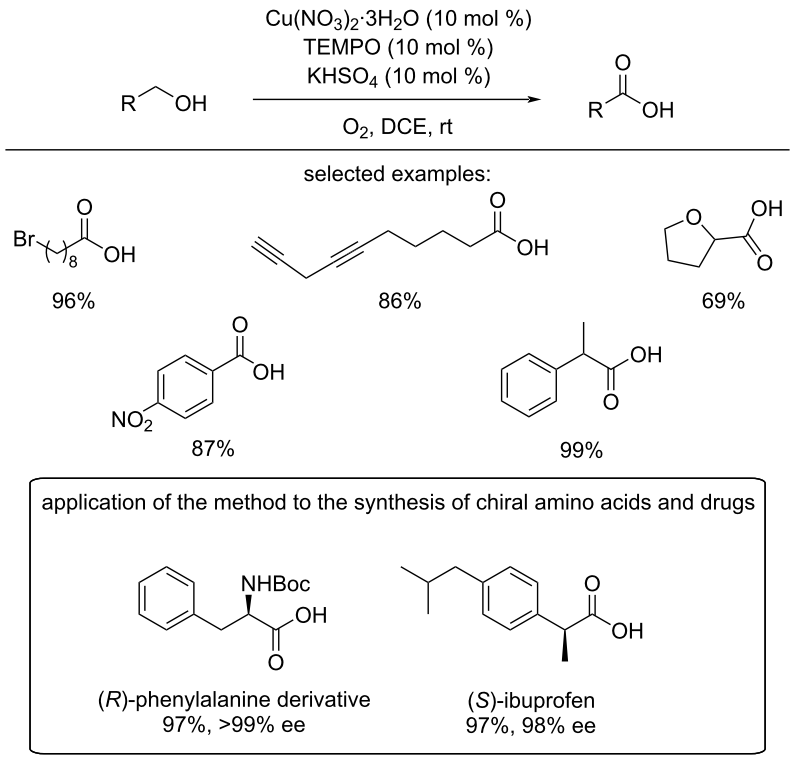
The most recent report on aerobic Cu-catalyzed oxidation of aldehydes, published in 2025 by the group of Ma, overcomes these disadvantages by offering an operationally simple ligand-free procedure that utilizes a cheap and readily available salt, namely $Cu(NO_3)_2{\cdot}3H_2O$, in combination with TEMPO as a co-catalyst [100]. The transformation proceeds under mild conditions in 1,2-dichloroethane (DCE) and tolerates an array of functional groups. Moreover, the approach was proved selective towards different aldehyde functionalities, and its utility was showcased in the transformation of structurally complex steroid molecules (Scheme 25).

The group of Ma also reported an approach in which primary alcohols were efficiently and directly oxidized to acids employing catalytic amounts of $Cu(NO_3)_2{\cdot}3H_2O$, TEMPO, and $KHSO_4$ under O_2 [101]. Alcohols containing aliphatic, benzylic, alkynyl, amino, as well as sterically demanding groups were readily oxidized in high isolated yields. In addition, starting from chiral alcohol precursors the synthesis of important amino acids and drugs was achieved without racemization (Scheme 26).

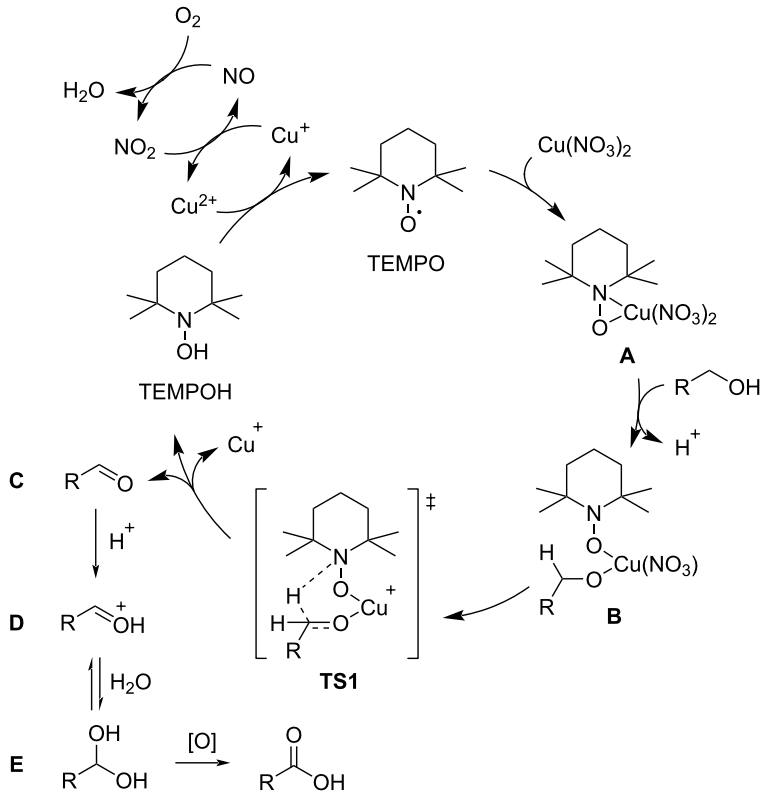
A mechanistic study showed that both bisulfate ($KHSO_4$) and water are essential for the reaction. The former facilitates the alcohol oxidation, whereas water ensures the hydration of the intermediate aldehyde, consequently accelerating the overall reaction [102]. The mechanism proposed by the group of Ma for the direct transformation of primary alcohols into acids is depicted in Scheme 27. First, intermediate **A** is formed from TEMPO and $Cu(NO_3)_2$, which then undergoes a



Scheme 25: $Cu(NO_3)_2{\cdot}3H_2O$/TEMPO-catalyzed selective oxidation of aldehydes.



Scheme 26: $Cu(NO_3)_2{\cdot}3H_2O$/TEMPO/$KHSO_4$-catalyzed direct oxidation of alcohols to carboxylic acids.



Scheme 27: Proposed mechanism for the $Cu(NO_3)_2{\cdot}3H_2O$/TEMPO/$KHSO_4$-catalyzed direct conversion of alcohols to acids.

ligand exchange with the alcohol substrate to generate **B**. Hydrogen-atom abstraction through the cyclic transition state **TS1** yields TEMPOH, Cu^{+}, and aldehyde **C**. Oxidation of TEMPOH by Cu^{2+} regenerates TEMPO, whereas Cu^{2+} is restored by oxidation of Cu^{+} with NO_2. Protonation of aldehyde **C** affords intermediate **D**, which is then hydrated to **E**. Finally, oxidation of *gem*-diol **E** via the same catalytic pathway as for the alcohol furnishes the carboxylic acid product [102].

Summary and Outlook

Copper-catalyzed aerobic oxidation of alcohols and aldehydes represents a highly valuable transformation in modern synthetic chemistry. A defining advantage of these reactions is the use of molecular oxygen as the terminal oxidant, offering excellent atom economy, low cost, and reduced environmental impact compared to traditional stoichiometric oxidants.

The success of these methodologies is closely linked to the accessibility and versatility of copper. Copper, as an earth-abundant transition metal, provides a sustainable alternative to noble metals while maintaining rich and tunable redox behavior. Its ability to operate within diverse catalytic systems, including those involving organic co-catalysts or ligand-assisted pathways, underpins the broad applicability of aerobic oxidation chemistry.

In the context of green chemistry, copper-catalyzed aerobic oxidation aligns well with key principles such as the use of benign oxidants, waste minimization, and the avoidance of toxic or precious metals, particularly when implemented under operationally simple conditions.

Despite the considerable progress achieved in this field, important challenges remain. Many of the reported systems rely on the presence of additional components such as nitroxyl mediators, tailored ligands, or basic additives, which can complicate reaction design and limit practical applicability. Recent advances, however, suggest that simpler catalytic systems, potentially operating in the absence of external mediators, ligands, and/or base additives, are within reach. These emerging examples underscore the need for continued efforts in catalyst discovery, systematic screening, and mechanistic investigation within the synthetic community.

Furthermore, the development of methodologies based on readily available, off-the-shelf reagents and catalysts should be considered a priority. In many practical settings, such systems are strongly preferred over in-house synthesized complexes, as they enhance the operational simplicity, reproducibility, and broader accessibility of the protocols. Progress along these lines is expected to further consolidate copper-catalyzed aerobic oxidation as a cornerstone transformation in sustainable organic synthesis.

Funding

This work received financial support from the Bulgarian National Science Fund (BNSF) under the National Scientific Program “VIHREN” (grant КП-06-ДВ-1).

Author Contributions

Hristo Petkov: conceptualization; writing – original draft. Svilen P. Simeonov: funding acquisition; writing – review & editing.

ORCID® iDs

Hristo Petkov - https://orcid.org/0000-0003-1829-0256

Data Availability Statement

Data sharing is not applicable as no new data was generated or analyzed in this study.

References

1. Gampe, C.; Verma, V. A. *J. Med. Chem.* **2020,** *63,* 14357–14381. doi:10.1021/acs.jmedchem.0c01177
2. Aljaafari, M. N.; Alkhoori, M. A.; Hag-Ali, M.; Cheng, W.-H.; Lim, S.-H.-E.; Loh, J.-Y.; Lai, K.-S. *Molecules* **2022,** *27,* 3589. doi:10.3390/molecules27113589
3. Catalano, A.; Mariconda, A.; D’Amato, A.; Iacopetta, D.; Ceramella, J.; Marra, M.; Saturnino, C.; Sinicropi, M. S.; Longo, P. *Organics* **2024,** *5,* 395–428. doi:10.3390/org5040021
4. Mushtaq, I.; Ahmad, M.; Saleem, M.; Ahmed, A. *Future J. Pharm. Sci.* **2024,** *10,* 16. doi:10.1186/s43094-024-00594-5
5. Sukhorukov, A. Y. *Front. Chem. (Lausanne, Switz.)* **2020,** *8,* 595246. doi:10.3389/fchem.2020.595246
6. Zeng, X.-P.; Sun, J.-C.; Liu, C.; Ji, C.-B.; Peng, Y.-Y. *Adv. Synth. Catal.* **2019,** *361,* 3281–3305. doi:10.1002/adsc.201900015
7. Dai, X.-J.; Li, C.-C.; Li, C.-J. *Chem. Soc. Rev.* **2021,** *50,* 10733–10742. doi:10.1039/d1cs00418b
8. Foley, D. J.; Waldmann, H. *Chem. Soc. Rev.* **2022,** *51,* 4094–4120. doi:10.1039/d2cs00101b
9. Narendar Reddy, T.; Beatriz, A.; Jayathirtha Rao, V.; de Lima, D. P. *Chem. – Asian J.* **2019,** *14,* 344–388. doi:10.1002/asia.201801560
10. Theodoropoulou, M. A.; Nikitas, N. F.; Kokotos, C. G. *Beilstein J. Org. Chem.* **2020,** *16,* 833–857. doi:10.3762/bjoc.16.76
11. Zou, K.; Deng, W.; Silvester, D. S.; Zou, G.; Hou, H.; Banks, C. E.; Li, L.; Hu, J.; Ji, X. *ACS Nano* **2024,** *18,* 19950–20000. doi:10.1021/acsnano.4c02307
12. Lawrence, N. J. *J. Chem. Soc., Perkin Trans. 1* **1998,** *27,* 1739–1750. doi:10.1039/a800646f
13. Cainelli, G.; Cardillo, G. *Chromium Oxidations in Organic Chemistry,* 1st ed.; Reactivity and Structure: Concepts in Organic Chemistry, Vol. 19; Springer-Verlag: Berlin, Heidelberg, Germany, 1984. doi:10.1007/978-3-642-69362-5
14. Dash, S.; Patel, S.; Mishra, B. K. *Tetrahedron* **2009,** *65,* 707–739. doi:10.1016/j.tet.2008.10.038

15. Tohma, H.; Kita, Y. *Adv. Synth. Catal.* **2004,** *346,* 111–124. doi:10.1002/adsc.200303203
16. Omura, K.; Swern, D. *Tetrahedron* **1978,** *34,* 1651–1660. doi:10.1016/0040-4020(78)80197-5
17. Corey, E. J.; Kim, C. U. *J. Am. Chem. Soc.* **1972,** *94,* 7586–7587. doi:10.1021/ja00776a056
18. Parikh, J. R.; Doering, W. v. E. *J. Am. Chem. Soc.* **1967,** *89,* 5505–5507. doi:10.1021/ja00997a067
19. Bal, B. S.; Childers, W. E., Jr.; Pinnick, H. W. *Tetrahedron* **1981,** *37,* 2091–2096. doi:10.1016/s0040-4020(01)97963-3
20. Tojo, G.; Fernández, M. *Oxidation of Alcohols to Aldehydes and Ketones, A Guide to Current Common Practice,* 1st ed.; Basic Reactions in Organic Synthesi; Springer Science and Business Media, Inc.: New York, USA, 2006. doi:10.1007/b135954
21. Punniyamurthy, T.; Rout, L. *Coord. Chem. Rev.* **2008,** *252,* 134–154. doi:10.1016/j.ccr.2007.04.003
22. Ballester, J.; Caminade, A.-M.; Majoral, J.-P.; Taillefer, M.; Ouali, A. *Catal. Commun.* **2014,** *47,* 58–62. doi:10.1016/j.catcom.2013.12.030
23. Herrerías, C. I.; Zhang, T. Y.; Li, C.-J. *Tetrahedron Lett.* **2006,** *47,* 13–17. doi:10.1016/j.tetlet.2005.10.123
24. Bauer, E. B. *Isr. J. Chem.* **2017,** *57,* 1131–1150. doi:10.1002/ijch.201700050
25. Ma, S.; Liu, J.; Li, S.; Chen, B.; Cheng, J.; Kuang, J.; Liu, Y.; Wan, B.; Wang, Y.; Ye, J.; Yu, Q.; Yuan, W.; Yu, S. *Adv. Synth. Catal.* **2011,** *353,* 1005–1017. doi:10.1002/adsc.201100033
26. Jiang, X.; Zhang, J.; Ma, S. *J. Am. Chem. Soc.* **2016,** *138,* 8344–8347. doi:10.1021/jacs.6b03948
27. Wang, L.; Shang, S.; Li, G.; Ren, L.; Lv, Y.; Gao, S. *J. Org. Chem.* **2016,** *81,* 2189–2193. doi:10.1021/acs.joc.6b00009
28. Jiang, X.; Liu, J.; Ma, S. *Org. Process Res. Dev.* **2019,** *23,* 825–835. doi:10.1021/acs.oprd.8b00374
29. Allen, S. E.; Walvoord, R. R.; Padilla-Salinas, R.; Kozlowski, M. C. *Chem. Rev.* **2013,** *113,* 6234–6458. doi:10.1021/cr300527g
30. Saranya, S.; Anilkumar, G. Copper Catalysis. In *Copper Catalysis in Organic Synthesis;* Saranya, S.; Anilkumar, G., Eds.; John Wiley & Sons: Weinheim, Germany,, 2020; pp 1–5. doi:10.1002/9783527826445.ch1
31. ICH Guideline Q3D (R2) on Elemental Impurities. European Medicines Agency (EMA), 2022; https://www.ema.europa.eu/en/documents/scientific-guideline/international-conference-harmonisation-technical-requirements-registration-pharmaceuticals-human-use-ich-q3d-elemental-impurities-step-5-revision-2_en.pdf (accessed Aug 19, 2026).
32. Zhu, X.; Chiba, S. *Chem. Soc. Rev.* **2016,** *45,* 4504–4523. doi:10.1039/c5cs00882d
33. Cheng, L.-J.; Mankad, N. P. *Chem. Soc. Rev.* **2020,** *49,* 8036–8064. doi:10.1039/d0cs00316f
34. Monnier, F.; Taillefer, M. *Angew. Chem., Int. Ed.* **2009,** *48,* 6954–6971. doi:10.1002/anie.200804497
35. Wendlandt, A. E.; Suess, A. M.; Stahl, S. S. *Angew. Chem., Int. Ed.* **2011,** *50,* 11062–11087. doi:10.1002/anie.201103945
36. Marais, L.; Vosloo, H. C. M.; Swarts, A. J. *Coord. Chem. Rev.* **2021,** *440,* 213958. doi:10.1016/j.ccr.2021.213958
37. Li, S.; An, Y.; Wang, L.; Chen, Y.; Huang, J.; Li, T.; Wen, B.; Chen, X. *ACS Omega* **2025,** *10,* 11454–11462. doi:10.1021/acsomega.4c11496
38. Gamez, P.; Aubel, P. G.; Driessen, W. L.; Reedijk, J. *Chem. Soc. Rev.* **2001,** *30,* 376–385. doi:10.1039/b104827a
39. Ryland, B. L.; Stahl, S. S. *Angew. Chem., Int. Ed.* **2014,** *53,* 8824–8838. doi:10.1002/anie.201403110
40. Marais, L.; Swarts, A. J. *Catalysts* **2019,** *9,* 395. doi:10.3390/catal9050395
41. Silva, T. F. S.; Martins, L. M. D. R. S. *Molecules* **2020,** *25,* 748. doi:10.3390/molecules25030748
42. Zhang, S.; Huang, W.; Fayad, E.; Nasser Binjawhar, D.; Rakesh, K. P.; Qin, H.-L. *Org. Biomol. Chem.* **2025,** *23,* 8128–8144. doi:10.1039/d5ob01174d
43. Forgione, P.; Bhattacharyya, D.; Oliveira de Paula, M.; Koscielniak, S. *SynOpen* **2026,** *10,* 66–77. doi:10.1055/a-2780-6932
44. Wang, C.; Xiao, J. *Acc. Chem. Res.* **2025,** *58,* 714–731. doi:10.1021/acs.accounts.4c00731
45. Liang, Y.; Wei, J.; Qiu, X.; Jiao, N. *Chem. Rev.* **2018,** *118,* 4912–4945. doi:10.1021/acs.chemrev.7b00193
46. McCann, S. D.; Stahl, S. S. *Acc. Chem. Res.* **2015,** *48,* 1756–1766. doi:10.1021/acs.accounts.5b00060
47. Feringa, B. L. Oxidation Catalysis; A Dinuclear Approach. In *Bioinorganic Chemistry of Copper;* Karlin, K. D.; Tyeklár, Z., Eds.; Springer: Dordrecht, Netherlands, 1993; pp 306–324. doi:10.1007/978-94-011-6875-5_24
48. Jacobson, R. R.; Tyeklar, Z.; Farooq, A.; Karlin, K. D.; Liu, S.; Zubieta, J. *J. Am. Chem. Soc.* **1988,** *110,* 3690–3692. doi:10.1021/ja00219a071
49. Garcia-Bosch, I.; Company, A.; Frisch, J. R.; Torrent-Sucarrat, M.; Cardellach, M.; Gamba, I.; Güell, M.; Casella, L.; Que, L., Jr.; Ribas, X.; Luis, J. M.; Costas, M. *Angew. Chem., Int. Ed.* **2010,** *49,* 2406–2409. doi:10.1002/anie.200906749
50. Kitajima, N.; Fujisawa, K.; Morooka, Y.; Toriumi, K. *J. Am. Chem. Soc.* **1989,** *111,* 8975–8976. doi:10.1021/ja00206a062
51. Zhang, C. X.; Liang, H.-C.; Kim, E.-i.; Shearer, J.; Helton, M. E.; Kim, E.; Kaderli, S.; Incarvito, C. D.; Zuberbühler, A. D.; Rheingold, A. L.; Karlin, K. D. *J. Am. Chem. Soc.* **2003,** *125,* 634–635. doi:10.1021/ja028779v
52. Jung, B.; Karlin, K. D.; Zuberbühler, A. D. *J. Am. Chem. Soc.* **1996,** *118,* 3763–3764. doi:10.1021/ja954157g
53. Karlin, K. D.; Tolman, W. B.; Kaderli, S.; Zuberbühler, A. D. *J. Mol. Catal. A: Chem.* **1997,** *117,* 215–222. doi:10.1016/s1381-1169(96)00250-6
54. Hatcher, L. Q.; Vance, M. A.; Sarjeant, A. A. N.; Solomon, E. I.; Karlin, K. D. *Inorg. Chem.* **2006,** *45,* 3004–3013. doi:10.1021/ic052185m
55. Das, O.; Paine, T. K. Copper Catalysts for Aerobic Oxidation of Alcohols. In *Transition Metal Catalysis in Aerobic Alcohol Oxidation;* Cardona, F.; Parmeggiani, C., Eds.; The Royal Society of Chemistry: Cambridge, U.K., 2014; pp 40–69. doi:10.1039/9781782621652-00040
56. Almasalma, A. A.; Mejía, E. Aerobic Cu-Catalyzed Organic Reactions. In *Copper Catalysis in Organic Synthesis;* Anilkumar, G.; Saranya, S., Eds.; Wiley-VCH Verlag GmbH & Co. KGaA: Weinheim, Germany, 2020; pp 349–366. doi:10.1002/9783527826445.ch16
57. Cao, Q.; Dornan, L. M.; Rogan, L.; Hughes, N. L.; Muldoon, M. J. *Chem. Commun.* **2014,** *50,* 4524–4543. doi:10.1039/c3cc47081d
58. Semmelhack, M. F.; Schmid, C. R.; Cortes, D. A.; Chou, C. S. *J. Am. Chem. Soc.* **1984,** *106,* 3374–3376. doi:10.1021/ja00323a064
59. Sheldon, R. A.; Arends, I. W. C. E. *J. Mol. Catal. A: Chem.* **2006,** *251,* 200–214. doi:10.1016/j.molcata.2006.02.016
60. Piera, J.; Bäckvall, J.-E. *Angew. Chem., Int. Ed.* **2008,** *47,* 3506–3523. doi:10.1002/anie.200700604
61. Gamez, P.; Arends, I. W. C. E.; Reedijk, J.; Sheldon, R. A. *Chem. Commun.* **2003,** 2414–2415. doi:10.1039/b308668b

62. Mannam, S.; Alamsetti, S. K.; Sekar, G. *Adv. Synth. Catal.* **2007,** *349,* 2253–2258. doi:10.1002/adsc.200700213
63. Hoover, J. M.; Stahl, S. S. *J. Am. Chem. Soc.* **2011,** *133,* 16901–16910. doi:10.1021/ja206230h
64. Steves, J. E.; Stahl, S. S. *J. Am. Chem. Soc.* **2013,** *135,* 15742–15745. doi:10.1021/ja409241h
65. Steves, J. E.; Stahl, S. S. *J. Org. Chem.* **2015,** *80,* 11184–11188. doi:10.1021/acs.joc.5b01950
66. Sasano, Y.; Nagasawa, S.; Yamazaki, M.; Shibuya, M.; Park, J.; Iwabuchi, Y. *Angew. Chem., Int. Ed.* **2014,** *53,* 3236–3240. doi:10.1002/anie.201309634
67. Sasano, Y.; Kogure, N.; Nagasawa, S.; Kasabata, K.; Iwabuchi, Y. *Org. Lett.* **2018,** *20,* 6104–6107. doi:10.1021/acs.orglett.8b02528
68. Hoover, J. M.; Ryland, B. L.; Stahl, S. S. *ACS Catal.* **2013,** *3,* 2599–2605. doi:10.1021/cs400689a
69. Mei, Q.; Liu, H.; Yang, Y.; Liu, H.; Li, S.; Zhang, P.; Han, B. *ACS Sustainable Chem. Eng.* **2018,** *6,* 2362–2369. doi:10.1021/acssuschemeng.7b03820
70. Lagerspets, E.; Abba, D.; Sharratt, J.; Eronen, A.; Repo, T. *Mol. Catal.* **2022,** *520,* 112167. doi:10.1016/j.mcat.2022.112167
71. Heshmatnia, F.; Zupanc, A.; Eronen, A.; Lagerspets, E.; Install, J.; Repo, T. *ChemSusChem* **2025,** *18,* e202402236. doi:10.1002/cssc.202402236
72. Zhai, D.; Ma, S. *Org. Chem. Front.* **2019,** *6,* 3101–3106. doi:10.1039/c9qo00740g
73. Jallabert, C.; Riviere, H. *Tetrahedron Lett.* **1977,** *18,* 1215–1218. doi:10.1016/s0040-4039(01)92978-8
74. Jallabert, C.; Riviere, H. *Tetrahedron* **1980,** *36,* 1191–1194. doi:10.1016/0040-4020(80)87017-7
75. Sakharov, A. M.; Skibida, I. P. *J. Mol. Catal.* **1988,** *48,* 157–174. doi:10.1016/0304-5102(88)85002-8
76. Liu, X.; Qiu, A.; Sawyer, D. T. *J. Am. Chem. Soc.* **1993,** *115,* 3239–3243. doi:10.1021/ja00061a023
77. Markó, I. E.; Giles, P. R.; Tsukazaki, M.; Brown, S. M.; Urch, C. J. *Science* **1996,** *274,* 2044–2046. doi:10.1126/science.274.5295.2044
78. Markó, I. E.; Gautier, A.; Dumeunier, R.; Doda, K.; Philippart, F.; Brown, S. M.; Urch, C. J. *Angew. Chem., Int. Ed.* **2004,** *43,* 1588–1591. doi:10.1002/anie.200353458
79. Markó, I. E.; Giles, P. R.; Tsukazaki, M.; Chellé-Regnaut, I.; Gautier, A.; Brown, S. M.; Urch, C. J. *J. Org. Chem.* **1999,** *64,* 2433–2439. doi:10.1021/jo982239s
80. McCann, S. D.; Stahl, S. S. *J. Am. Chem. Soc.* **2016,** *138,* 199–206. doi:10.1021/jacs.5b09940
81. Xu, B.; Lumb, J.-P.; Arndtsen, B. A. *Angew. Chem., Int. Ed.* **2015,** *54,* 4208–4211. doi:10.1002/anie.201411483
82. McCann, S. D.; Lumb, J.-P.; Arndtsen, B. A.; Stahl, S. S. *ACS Cent. Sci.* **2017,** *3,* 314–321. doi:10.1021/acscentsci.7b00022
83. Zhan, L.-W.; Han, L.; Xing, P.; Jiang, B. *Org. Lett.* **2015,** *17,* 5990–5993. doi:10.1021/acs.orglett.5b02756
84. Hu, J.; Zhu, Y.; Gao, H.; Zhang, F.; Zhang, Z. *Ind. Eng. Chem. Res.* **2022,** *61,* 13408–13415. doi:10.1021/acs.iecr.2c02413
85. Greene, J. F.; Hoover, J. M.; Mannel, D. S.; Root, T. W.; Stahl, S. S. *Org. Process Res. Dev.* **2013,** *17,* 1247–1251. doi:10.1021/op400207f
86. Greene, J. F.; Preger, Y.; Stahl, S. S.; Root, T. W. *Org. Process Res. Dev.* **2015,** *19,* 858–864. doi:10.1021/acs.oprd.5b00125
87. Urch, C. J.; Marko, I. E.; Tuskazaki, M.; Giles, P. R.; Brown, S. M. Preparation of aldehydes or ketones from alcohols. U.S. Patent 5,912,388, June 15, 1999.
88. DSM Fine Chemicals Austria NFG GMBH & Co. KG. Verfahren zur Herstellung von Aldehyden aus Alkoholen durch Cu - katalysierte Oxidation. Austrian Pat. Appl. AT501929(A1), Dec 15, 2006.
89. Hansen, T. S.; Sádaba, I.; García-Suárez, E. J.; Riisager, A. *Appl. Catal., A* **2013,** *456,* 44–50. doi:10.1016/j.apcata.2013.01.042
90. Tong, X.; Sun, Y.; Bai, X.; Li, Y. *RSC Adv.* **2014,** *4,* 44307–44311. doi:10.1039/c4ra07181f
91. Li, X.-L.; Qing, S.-J.; Sun, X.; Yu, Z.; Xu, H.-J.; Fu, Y. *ChemSusChem* **2025,** *18,* e202401527. doi:10.1002/cssc.202401527
92. Zheng, S.; Smit, W.; Spannenberg, A.; Tin, S.; de Vries, J. G. *Chem. Commun.* **2022,** *58,* 4639–4642. doi:10.1039/d2cc00773h
93. Petkov, H.; Ravutsov, M. A.; Verganista, M. J.; Mitrev, Y. N.; Candeias, N. R.; Simeonov, S. P. *ChemSusChem* **2024,** *17,* e202400013. doi:10.1002/cssc.202400013
94. Spang, J.; Mascia, F.; Kroutil, W. *JACS Au* **2026,** *6,* 659–677. doi:10.1021/jacsau.5c01452
95. Besson, M.; Gallezot, P. *Catal. Today* **2000,** *57,* 127–141. doi:10.1016/s0920-5861(99)00315-6
96. Biella, S.; Prati, L.; Rossi, M. *J. Mol. Catal. A: Chem.* **2003,** *197,* 207–212. doi:10.1016/s1381-1169(02)00618-0
97. Liu, M.; Wang, H.; Zeng, H.; Li, C.-J. *Sci. Adv.* **2015,** *1,* e1500020. doi:10.1126/sciadv.1500020
98. Liu, M.; Li, C.-J. *Angew. Chem., Int. Ed.* **2016,** *55,* 10806–10810. doi:10.1002/anie.201604847
99. Xu, S.; Zhang, X.; Xiong, W.; Li, P.; Ma, W.; Hu, X.; Wu, Y. *Chem. Commun.* **2022,** *58,* 2132–2135. doi:10.1039/d1cc04812k
100. Huang, Y.; Jiang, S.; Zhou, Z.; Yu, Y.; Qian, H.; Ma, S. *Org. Chem. Front.* **2025,** *12,* 4980–4985. doi:10.1039/d5qo00330j
101. Yu, Y.; Zhai, D.; Zhou, Z.; Jiang, S.; Qian, H.; Ma, S. *Chem. Commun.* **2023,** *59,* 5281–5284. doi:10.1039/d3cc00963g
102. Yu, Y.; Sun, Z.; Guo, Y.-L.; Zhang, X.; Qian, H.; Ma, S. *Org. Chem. Front.* **2024,** *11,* 5003–5009. doi:10.1039/d4qo00791c

License and Terms

This is an open access article licensed under the terms of the Beilstein-Institut Open Access License Agreement (https://www.beilstein-journals.org/bjoc/terms), which is identical to the Creative Commons Attribution 4.0 International License (https://creativecommons.org/licenses/by/4.0). The reuse of material under this license requires that the author(s), source and license are credited. Third-party material in this article could be subject to other licenses (typically indicated in the credit line), and in this case, users are required to obtain permission from the license holder to reuse the material.

The definitive version of this article is the electronic one which can be found at:
https://doi.org/10.3762/bjoc.22.107